

On the Statistical Complexity of Estimating Vendi Scores from Empirical Data

Azim Ospanov*, Farzan Farnia†

Abstract

Evaluating the diversity of generative models without access to reference data poses methodological challenges. The reference-free Vendi score [1] offers a solution by quantifying the diversity of generated data using matrix-based entropy measures. The Vendi score is usually computed via the eigendecomposition of an $n \times n$ kernel matrix for n generated samples. However, the heavy computational cost of eigendecomposition for large n often limits the sample size used in practice to a few tens of thousands. In this paper, we investigate the statistical convergence of the Vendi score. We numerically demonstrate that for kernel functions with an infinite feature map dimension, the score estimated from a limited sample size may exhibit a non-negligible bias relative to the population Vendi score, i.e., the asymptotic limit as the sample size approaches infinity. To address this, we introduce a truncation of the Vendi statistic, called the *t-truncated Vendi statistic*, which is guaranteed to converge to its asymptotic limit given $n = O(t)$ samples. We show that the existing Nyström method and the FKEA approximation method for approximating the Vendi score both converge to the population truncated Vendi score. We perform several numerical experiments to illustrate the concentration of the Nyström and FKEA-computed Vendi scores around the truncated Vendi and discuss how the truncated Vendi score correlates with the diversity of image and text data.

1 Introduction

The increasing use of generative artificial intelligence has highlighted the need for accurate evaluation of generative models, particularly in terms of sample quality and diversity. In practice, users often have access to multiple generative models trained on different datasets using various algorithms, necessitating efficient evaluation methods to identify the most suitable model. The feasibility of a model evaluation approach depends on factors such as the required generated sample size, computational cost, and the availability of reference data. Recent studies on evaluating generative models have introduced assessment methods that relax the requirements on data and computational resources.

Specifically, to enable the evaluation of generative models in settings without reference data, the recent literature has focused on reference-free evaluation scores, which remain applicable in the absence of a reference dataset. The Vendi score [1] is one such reference-free metric that quantifies the diversity of generated data using the entropy of a kernel similarity matrix formulated for the generated samples. As analyzed by [1] and [2], the reference-free assessment of the Vendi score can be interpreted as an unsupervised identification of clusters within the generated data, followed by the calculation of the entropy of the detected cluster variable. Due to its flexibility and adaptability to various domains, the Vendi score has been applied to measure the diversity of samples across different modalities, including image, text, and video data.

While the Vendi score does not require reference samples, its computational cost increases rapidly with the number of generated samples n . In practice, calculating the entropy of the eigenvalues of the $n \times n$ kernel matrix involves performing an eigendecomposition, which requires $O(n^3)$ computations. As a result, the computational load becomes substantial for a large sample size n , and the Vendi score is typically evaluated

*Department of Computer Science and Engineering, The Chinese University of Hong Kong, aospanov9@cse.cuhk.edu.hk

†Department of Computer Science and Engineering, The Chinese University of Hong Kong, farnia@cse.cuhk.edu.hk

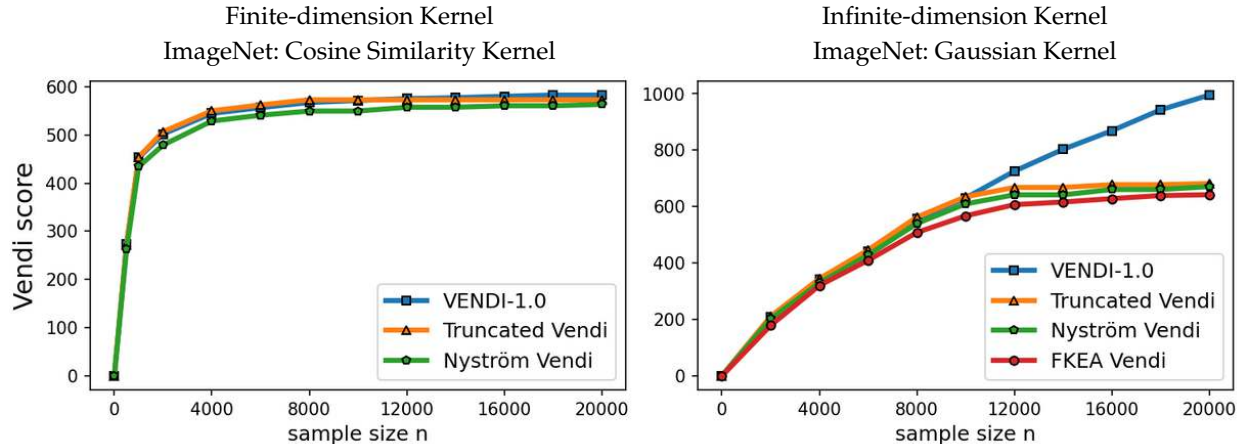


Figure 1: Statistical convergence of Vendi score for different sample sizes on ImageNet data: (Left plot) finite-dimension cosine similarity kernel (Right plot) infinite dimension Gaussian kernel with bandwidth $\sigma = 40$. DINOv2 embedding (dimension 768) is used in computing the score.

for sample sizes limited to a few tens of thousands. Consequently, the exact Vendi score, as defined in its original formulation, is usually not computed for sample sizes exceeding 20,000. A key question that arises is whether the Vendi score estimated from empirical data has converged to the population Vendi score, i.e., the limit value of the score when the sample size approaches infinity. The statistical convergence of Vendi scores has not been thoroughly investigated for models trained on large-scale datasets, e.g. ImageNet [3] and MS COCO [4], which contain many sample categories and may require a large sample size for proper assessment.

In this work, we study the statistical convergence of the Vendi score and aim to analyze the concentration of the estimated Vendi scores for large-scale image, text, and video generative models. We discuss the answer to the convergence question for two types of kernel functions: 1) kernel functions with a finite feature dimension, e.g. the cosine similarity and polynomial kernels, 2) kernel functions with an infinite feature map such as Gaussian (RBF) and Laplace kernels. For kernel functions with a finite feature dimension d , we theoretically and numerically show that a sample size $n = O(d)$ is sufficient to guarantee convergence to the population Vendi score (asymptotic limit when $n \rightarrow \infty$). For example, the left plot in Figure 1 shows that in the case of the cosine similarity kernel, the Vendi score on n randomly selected ImageNet samples has almost converged as the sample size reaches 5000, where the dimension d (using standard DINOv2 embedding [5]) is 768.

On the other hand, our numerical results for kernel functions with an infinite feature map suggest that in practical scenarios with diverse generative models and datasets, a sample size bounded by 20,000 could be insufficient for convergence to the population Vendi score. For example, the right plot in Figure 1 shows the evolution of the Vendi score with Gaussian kernel on the ImageNet data, and the Vendi score keeps growing at a considerable rate even with 20,000 samples. As the costs of computing the exact score will be highly expensive beyond 20,000, it will be hard to empirically estimate the required sample size for convergence to the population Vendi.

Observing the difference between Vendi score for $n = O(10^4)$ and the population Vendi (as $n \rightarrow \infty$) under an infinite kernel feature dimension, a natural question is how to interpret the statistic estimated by the Vendi score from a restricted sample size n . We attempt to address the question by introducing an alternative population quantity, which we call the *t-truncated population Vendi*. This quantity is calculated using only the top- t eigenvalues of the kernel covariance matrix, excluding the remaining eigenvalues in the calculation of the population Vendi. We prove that a sample size $n = O(t)$ is always enough to estimate the *t-truncated* population Vendi from n generated samples, regardless of the finiteness of the kernel feature dimension. This

result shows that the t -truncated Vendi score offers a statistically affordable extension of the Vendi score from the finite kernel dimension to the infinite dimension case.

To connect the defined t -truncated Vendi score to existing computation methods for the Vendi score, we show that the standard methods proposed for computing the Vendi score can be viewed as estimations of the t -truncated population Vendi. First, we observe that the t -truncated Vendi score is identical to the Vendi score when the kernel feature dimension d is finite and bounded by t . Next, we show that the existing approximation methods, including the Nyström method [1] and the random Fourier feature-based FKEA method [6], also provide an estimate of the population t -truncated Vendi score. Therefore, our theoretical results suggest that the population truncated Vendi is implicitly estimated by the computationally efficient methods proposed by [1] and [6].

We perform several numerical experiments to validate the connection between the Vendi scores computed using a bounded n samples and our defined t -truncated population Vendi. Our numerical results on standard image, text, and video datasets and generative models indicate that in the case of a finite-dimension kernel map, the Vendi score efficiently converges to the population Vendi, which is identical to the truncated Vendi in the finite dimension case. On the other hand, in the case of infinite-dimension Gaussian kernel functions, we numerically observe the growth of the score beyond $n = 10,000$. Our numerical results further confirm that the scores computed by Nyström method in [1] and the FKEA method [6] provide tight estimations of the population truncated Vendi. The following summarizes this work’s contributions:

- Analyzing the statistical convergence of the reference-free Vendi score under finite and infinite kernel feature maps,
- Providing numerical evidence on the gap between the Vendi score and population Vendi for infinite kernel feature maps with bounded sample size n ,
- Introducing truncated Vendi score as a statistically affordable extension of the Vendi score from finite to infinite kernel feature dimensions,
- Demonstrating convergence of Nyström and FKEA proxy Vendi scores to population truncated Vendi score.

2 Related Works

Diversity evaluation for generative models Diversity evaluation in generative models can be categorized into two primary types: reference-based and reference-free methods. Reference-based approaches rely on a predefined dataset to assess the diversity of generated data. Metrics such as FID [7] and KID [8] measure the distance between the generated data and the reference, while Recall [9, 10] and Coverage [11] evaluate the extent to which the generative model captures existing modes in the reference dataset. [12, 13] propose MAUVE metric that uses information divergences in a quantized embedding space to measure the gap between generated data and reference distribution. In contrast, the reference-free metrics, Vendi [1][14] and RKE [2], assign diversity scores based on the eigenvalues of a kernel similarity matrix of the generated data. [2]’s results interpret the approach as identifying modes and their frequencies within the generated data followed by entropy calculation for the frequency parameters. In this work, we specifically focus on the statistical convergence of the reference-free Vendi and RKE scores.

Statistical convergence analysis of kernel matrices’ eigenvalues. The convergence analysis of the eigenvalues of kernel matrices has been studied by several related works. [15] provide a concentration bound for the eigenvalues of a kernel matrix. We note that the bounds in [15] use the expectation of eigenvalues $\mathbb{E}_m[\hat{\lambda}(S)]$ for a random dataset $S = (\mathbf{x}_1, \dots, \mathbf{x}_m)$ of fixed size m as the center vector in the concentration analysis. However, since eigenvalues are non-linear functions of a matrix, this concentration center vector $\mathbb{E}_m[\hat{\lambda}(S)]$ does not match the eigenvalues of the asymptotic kernel matrix as the sample size approaches to infinity. On the other hand, our convergence analysis focuses on the asymptotic eigenvalues with an infinite sample size, which determines the limit value of Vendi scores. In another related work, [16] discusses a convergence result for the Von-Neumann entropy of kernel matrix. While this result proves a non-asymptotic

guarantee on the convergence of the entropy function, the bound may not guarantee convergence at standard sample sizes for computing Vendi scores (less than 10000 in practice). In our work, we aim to provide convergence guarantees for the finite-dimension and generally truncated Vendi scores with restricted sample sizes.

Efficient computation of matrix-based entropy. Several strategies have been proposed in the literature to reduce the computational complexity of matrix-based entropy calculations, which involve the computation of matrix eigenvalues—a process that scales cubically with the size of the dataset. [17] propose an efficient algorithm for approximating matrix-based Renyi’s entropy of arbitrary order α , which achieves a reduction in computational complexity down to $O(n^2sm)$ with $s, m \ll n$. Additionally, kernel matrices can be approximated using low-rank techniques such as incomplete Cholesky decomposition [18, 19] or CUR matrix decompositions [20], which provide substantial computational savings. [14] suggest to leverage Nyström method [21] with m components, which results in $O(nm^2)$ computational complexity. Further reduction in complexity is possible using Random Fourier Features, as suggested by [6], which allows the computation to scale linearly with $O(n)$ as a function of the dataset size. This work focuses on the latter two methods and the population quantities estimated by them.

Impact of embedding spaces on diversity evaluation. In our image-related experiments, we used the DinoV2 embedding [5], as [22] demonstrate the alignment of this embedding with human evaluations. We note that the kernel function in the Vendi score can be similarly applied to other embeddings, including the standard InceptionV3[23] and CLIP embeddings [24] as suggested by [25]. Also, in our experiments on text data, we utilized the text-embedding-3-large [26] model, and for the video experiments, we employed the I3D embedding [27]. We use the mentioned embeddings in our experiments, while our theoretical results suggest that the convergence behavior would be similar for other embeddings.

3 Preliminaries

Consider a generative model \mathcal{G} that generates samples from a probability distribution P_X . To conduct a reference-free evaluation of the model, we suppose the evaluator has access to n independently generated samples from P_X , denoted by $x_1, \dots, x_n \in \mathcal{X}$. The assessment task is to estimate the diversity of generative model \mathcal{G} by measuring the variety of the observed generated data, x_1, \dots, x_n . In the following subsections, we will discuss kernel functions and their application to define the Vendi diversity score.

3.1 Kernel Functions and Matrices

Following the standard definition, $k : \mathcal{X} \times \mathcal{X} \rightarrow \mathbb{R}$ is called a kernel function if for every integer n and inputs $x_1, \dots, x_n \in \mathcal{X}$, the kernel similarity matrix $K = [k(x_i, x_j)]_{1 \leq i, j \leq n}$ is positive semi-definite. Aronszajn’s Theorem [28] shows that this definition is equivalent to the existence of a feature map $\phi : \mathcal{X} \rightarrow \mathbb{R}^d$ such that for every $x, x' \in \mathcal{X}$ we have the following where $\langle \cdot, \cdot \rangle$ denotes the standard inner product in the \mathbb{R}^d space:

$$k(x, x') = \langle \phi(x), \phi(x') \rangle \tag{1}$$

In this work, we study the evaluation using two types of kernel functions: 1) finite-dimension kernels where dimension d is finite, 2) infinite-dimension kernels where there is no feature map satisfying (1) with a finite d value. A standard example of a finite-dimension kernel is the cosine similarity function where $\phi_{\text{cosine}}(x) = x/\|x\|_2$. Also, a widely-used infinite-dimension kernel is the Gaussian (RBF) kernel with bandwidth parameter $\sigma > 0$ defined as

$$k_{\text{Gaussian}(\sigma)}(x, x') := \exp\left(-\frac{\|x - x'\|_2^2}{2\sigma^2}\right) \tag{2}$$

Both the mentioned kernel examples belong to normalized kernels which require $k(x, x) = 1$ for every x , i.e. the feature map $\phi(x)$ has unit Euclidean norm for every x . Given a normalized kernel function, the non-negative eigenvalues of the normalized kernel matrix $\frac{1}{n}K$ for n points x_1, \dots, x_n will sum up to 1, which means that they form a probability model.

3.2 Matrix-based Entropy Functions and Vendi Score

Given a PSD matrix $A \in \mathbb{R}^{d \times d}$ with a unit trace $\text{Tr}(A) = 1$, A 's eigenvalues form a probability model. The order- α Renyi entropy of matrix A is defined using the order- α entropy of its eigenvalues as

$$H_\alpha(A) := \frac{1}{1-\alpha} \log\left(\sum_{i=1}^d \lambda_i^\alpha\right) \quad (3)$$

In the case of $\alpha = 1$, the above definition reduces to the Shannon entropy of the eigenvalues as $H_1(A) := \sum_{i=1}^d \lambda_i \log(1/\lambda_i)$ [29]. Applying the above standard definitions to the normalized kernel matrix $\frac{1}{n}K$, [14] define the order- α Vendi score for samples x_1, \dots, x_n as

$$\text{Vendi}_\alpha(x_1, \dots, x_n) := \exp\left(H_\alpha\left(\frac{1}{n}K\right)\right) \quad (4)$$

We note that in the case of $\alpha = 2$, the definition of Vendi_2 is identical to the RKE score proposed by [2]. In this particular case, the score can be formulated using the Frobenius norm of the kernel matrix, denoted by $\|\cdot\|_F$,

$$\text{RKE}(x_1, \dots, x_n) = \text{Vendi}_2(x_1, \dots, x_n) = \left\|\frac{1}{n}K\right\|_F^{-2}$$

3.3 Statistical Analysis of Vendi Score

To derive the population Vendi that is supposed to be estimated by the Vendi score, we review the following discussion from [16, 1, 2]. First, note that the normalized kernel matrix $\frac{1}{n}K$, whose eigenvalues are used in the definition of Vendi score, can be written as:

$$\frac{1}{n}K = \frac{1}{n}\Phi\Phi^\top \quad (5)$$

where $\Phi \in \mathbb{R}^{n \times d}$ is an $n \times d$ matrix whose rows are the feature presentations of samples, i.e., $\phi(x_1), \dots, \phi(x_n)$. Therefore, the normalized kernel matrix $\frac{1}{n}K$ shares the same non-zero eigenvalues with $\frac{1}{n}\Phi^\top\Phi$, in which the multiplication order is flipped. Note that $\frac{1}{n}\Phi^\top\Phi$ is defined as the empirical kernel covariance matrix C_X :

$$C_X := \frac{1}{n} \sum_{i=1}^n \phi(x_i)\phi(x_i)^\top = \frac{1}{n}\Phi^\top\Phi.$$

As a result, the empirical covariance matrix C_X and kernel matrix $\frac{1}{n}K$ have the same non-zero eigenvalues and therefore share the same matrix-based entropy value for any order α : $H_\alpha(\frac{1}{n}K) = H_\alpha(C_X)$. Therefore, if we consider the population kernel covariance matrix $\tilde{C}_X = \mathbb{E}_{x \sim P_X}[\phi(x)\phi(x)^\top]$, we can define the population Vendi score as follows.

Definition 1. Given data distribution P_X , we define the order- α population Vendi, $\text{Vendi}_\alpha(P_X)$, using the matrix-based entropy of the population kernel covariance matrix $\tilde{C}_X = \mathbb{E}_{x \sim P_X}[\phi(x)\phi(x)^\top]$ as

$$\text{Vendi}_\alpha(P_X) := \exp\left(H_\alpha(\tilde{C}_X)\right) \quad (6)$$

In the next sections, we study the complexity of estimating the above population Vendi from a limited number of samples.

4 Statistical Convergence of Vendi Scores in Finite-Dimension Kernels

Given the definitions of the Vendi score and the population Vendi, a relevant question is how many samples are required to accurately estimate the population Vendi using the Vendi score. To address this question, we first prove the following concentration bound on the vector of ordered eigenvalues $[\lambda_1, \dots, \lambda_n]$ of the kernel matrix for a normalized kernel function.

Theorem 1. *Consider a normalized kernel function k satisfying $k(x, x) = 1$ for every $x \in \mathcal{X}$. Let $\widehat{\lambda}_n$ be the vector of sorted eigenvalues of the normalized kernel matrix $\frac{1}{n}K$ for n independent samples $x_1, \dots, x_n \sim P_X$. If we define $\widetilde{\lambda}$ as the vector of sorted eigenvalues of underlying covariance matrix \widetilde{C}_X , then if $n \geq 2 + 8 \log(1/\delta)$, the following inequality holds with probability at least $1 - \delta$:*

$$\|\widehat{\lambda}_n - \widetilde{\lambda}\|_2 \leq \sqrt{\frac{32 \log(2/\delta)}{n}}$$

Note that in calculating the subtraction $\widehat{\lambda}_n - \widetilde{\lambda}$, we add $|d - n|$ zero entries to the lower-dimension vector, if the dimension of vectors $\widehat{\lambda}_n$ and $\widetilde{\lambda}$ do not match.

Proof. We defer the proof to the Appendix. □

The above theorem implies the following corollary on a dimension-dependent convergence guarantee for order- α Vendi score with $1 \leq \alpha < 2$.

Corollary 1. *In the setting of Theorem 1, consider a finite dimension kernel map where we suppose $\dim(\phi) = d < \infty$. (a) For $\alpha = 1$, assuming $n \geq 32e^2 \log(2/\delta)$, the following bound holds with probability at least $1 - \delta$:*

$$\begin{aligned} & \left| \log(\text{Vendi}_1(x_1, \dots, x_n)) - \log(\text{Vendi}_1(P_X)) \right| \\ & \leq \sqrt{\frac{8d \log(2/\delta)}{n}} \log\left(\frac{nd}{32 \log(2/\delta)}\right). \end{aligned}$$

(b) For every $1 < \alpha < 2$ and $n \geq 2 + 8 \log(1/\delta)$, the following bound holds with probability at least $1 - \delta$:

$$\begin{aligned} & \left| \text{Vendi}_\alpha(x_1, \dots, x_n)^{\frac{1-\alpha}{\alpha}} - \text{Vendi}_\alpha(P_X)^{\frac{1-\alpha}{\alpha}} \right| \\ & \leq \sqrt{\frac{32d^{2-\alpha} \log(2/\delta)}{n}} \end{aligned}$$

Note that the above concentration guarantee holds under a finite feature map dimension when $\alpha < 2$. On the other hand, the next corollary provides a dimension-independent convergence guarantee for the Vendi_α score with order $\alpha \geq 2$, suggesting a dimension-free concentration for the order 2 (i.e., RKE score) and above.

Corollary 2. *In the setting of Theorem 1, for every $\alpha \geq 2$ and $n \geq 2 + 8 \log(1/\delta)$, the following bound holds with probability at least $1 - \delta$:*

$$\begin{aligned} & \left| \text{Vendi}_\alpha(x_1, \dots, x_n)^{\frac{1-\alpha}{\alpha}} - \text{Vendi}_\alpha(P_X)^{\frac{1-\alpha}{\alpha}} \right| \\ & \leq \sqrt{\frac{32 \log(2/\delta)}{n}} \end{aligned}$$

Proof. We defer the proof to the Appendix. □

Therefore, assuming a bounded feature map $d < \infty$ and $1 \leq \alpha < 2$, the above results indicate the convergence of the Vendi score to the underlying population Vendi given $n = O(d^{2-\alpha})$ samples. We note that the result is consistent with our numerical observations of the convergence of Vendi score using a finite dimension kernel, e.g. the cosine similarity kernel (Figure 1). Next, we discuss how to extend the above result to an infinite-dimension kernel map by defining the truncated population Vendi.

5 Truncated Vendi Statistic and its Estimation via Proxy Kernels

Corollaries 1,2 demonstrate that if the Vendi score order α is greater than 2 or the kernel feature map dimension d is finite, then the Vendi score can converge to the population Vendi with $n = O(d)$ samples. However, the theoretical results do not apply to an order $1 \leq \alpha < 2$ when the kernel map dimension is infinite, e.g. the original order-1 Vendi score [1] with a Gaussian kernel. Our numerical observations indicate that a standard sample size below 20000 could be insufficient for the convergence of order-1 Vendi score (Figure 1). To address this gap, here we define the truncated population Vendi and then show the existing kernel approximation algorithms for Vendi score concentrate around this modified statistic.

Definition 2. Consider data distribution P and its underlying kernel covariance matrix $\tilde{C}_X = \mathbb{E}_{x \sim P} [\phi(x)\phi(x)^\top]$. Then, for parameter $t \geq 1$, consider the top- t eigenvalues of \tilde{C}_X : $\lambda_1 \geq \lambda_2 \geq \dots \geq \lambda_t$. Define $S_t = \sum_{i=1}^t \lambda_i$, and consider the probability sequence $\tilde{\lambda}_i = \lambda_i + \frac{1-S_t}{t}$ for $i = 1, \dots, t$. Then, we define the order- α t -truncated population Vendi as

$$\text{Vendi}_\alpha^{(t)}(P_X) := \exp\left(\frac{1}{1-\alpha} \log\left(\sum_{i=1}^t \tilde{\lambda}_i^\alpha\right)\right).$$

Remark 1. The above definition of t -truncated population Vendi, which is a function of underlying distribution P_X , motivates the definition of the t -truncated Vendi statistic $\text{Vendi}_\alpha^{(t)}(x_1, \dots, x_n)$ for empirical samples x_1, \dots, x_n , where we consider the empirical kernel covariance matrix $\hat{C}_X = \frac{1}{n} \sum_{i=1}^n \phi(x_i)\phi(x_i)^\top$. Note that the truncated Vendi statistic is a function of random samples x_1, \dots, x_n , while the truncated population Vendi depends only on P_X .

According to Definition 2, we find the probability model with the minimum ℓ_2 -norm difference from the t -dimensional vector $[\lambda_1, \dots, \lambda_t]$ including only the top- t eigenvalues. Then, we use the order- α entropy of the probability model to define the order- α t -truncated population Vendi. Our next result shows that this population quantity can be estimated using $n = O(t)$ samples by its empirical version, i.e., the t -truncated Vendi statistic in Remark 1.

Theorem 2. Consider the setting in Theorem 1. Then, for every $n \geq 2 + 8 \log(1/\delta)$, the difference between the t -truncated population Vendi and its empirical estimation from samples x_1, \dots, x_n (i.e. t -truncated Vendi statistic) is bounded with probability at least $1 - \delta$:

$$\begin{aligned} & \left| \text{Vendi}_\alpha^{(t)}(x_1, \dots, x_n)^{\frac{1-\alpha}{\alpha}} - \text{Vendi}_\alpha^{(t)}(P_X)^{\frac{1-\alpha}{\alpha}} \right| \\ & \leq \sqrt{\frac{32 \max\{1, t^{2-\alpha}\} \log(2/\delta)}{n}} \end{aligned}$$

Proof. We defer the proof to the Appendix. □

As implied by Theorem 2, the t -truncated population Vendi can be estimated using $O(t)$ samples, i.e. the truncation parameter t plays the role of the bounded dimension of a finite-dimension kernel map. Our next theorem shows that the Nyström method [14] and the FKEA method [6] for reducing the computational costs of Vendi scores have a bounded difference with the truncated population Vendi.

Theorem 3. Consider the setting of Theorem 1. (a) Assume that the kernel function is shift-invariant and the FKEA method with t random Fourier features is used to approximate the Vendi score. Then, for every δ satisfying $n \geq 2 + 8 \log(1/\delta)$, with probability at least $1 - \delta$:

$$\begin{aligned} & \left| \text{FKEA-Vendi}_\alpha^{(t)}(x_1, \dots, x_n)^{\frac{1-\alpha}{\alpha}} - \text{Vendi}_\alpha^{(t)}(P_X)^{\frac{1-\alpha}{\alpha}} \right| \\ & \leq \sqrt{\frac{128 \max\{1, t^{2-\alpha}\} \log(3/\delta)}{\min\{n, t\}}} \end{aligned}$$

(b) Assume that the Nyström method is applied with parameter t for approximating the kernel function. Then, if for some $r \geq 1$, the kernel matrix K 's r th-largest eigenvalue satisfies $\lambda_r \leq \tau$ and $t \geq r\tau \log(n)$, the following holds with probability at least $1 - \delta - 2n^{-3}$:

$$\begin{aligned} & \left| \text{Nyström-Vendi}_\alpha^{(t)}(x_1, \dots, x_n)^{\frac{1-\alpha}{\alpha}} - \text{Vendi}_\alpha^{(t)}(P_X)^{\frac{1-\alpha}{\alpha}} \right| \\ & \leq \mathcal{O}\left(\sqrt{\frac{\max\{1, t^{2-\alpha}\} \log(2/\delta) t \tau^2 \log(n)^2}{n}}\right) \end{aligned}$$

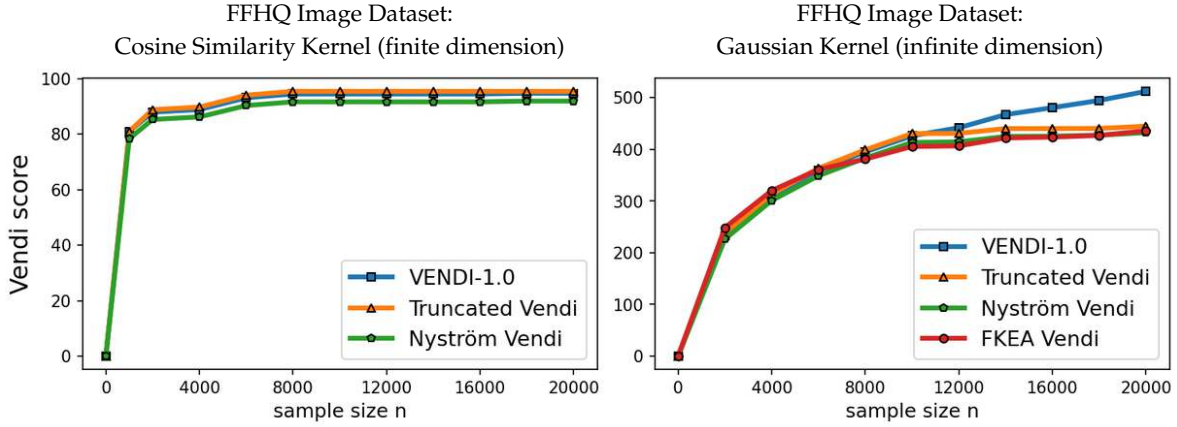
Proof. We defer the proof to the Appendix. □

6 Numerical Results

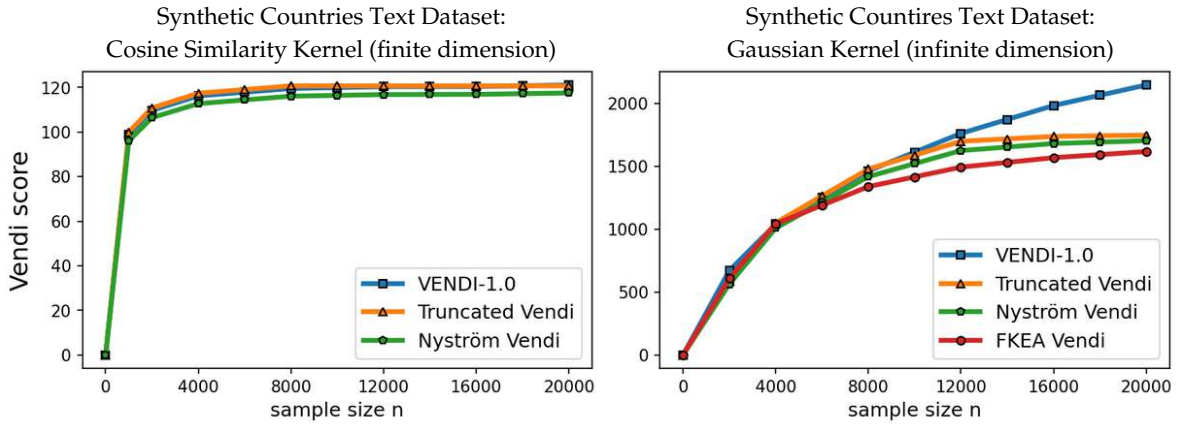
We evaluated the convergence of the Vendi score, the truncated Vendi score, and the proxy Vendi scores using the Nyström method and FKEA in our numerical experiments. We provide a comparative analysis of these scores across different data types and models, including image, text, and video. In our experiments, we considered the cosine similarity kernel as a standard kernel function with a finite-dimension map and the Gaussian (RBF) kernel as a kernel function with an infinite-dimension feature map. In the experiments with Gaussian kernels, we matched the kernel bandwidth parameter with those chosen by [2, 6] for the same datasets. We used 20,000 number of samples per score computation, consistent with standard practice in the literature. To investigate how computation-cutting methods compare to each other, in the experiments we matched the truncation parameter t of our defined t -truncated Vendi score with the Nyström method's hyperparameter on the number of randomly selected rows of kernel matrix and the FKEA's hyperparameter of the number of random Fourier features. The Vendi and FKEA implementations were adopted from the corresponding references' GitHub webpages, while the Nyström method was adopted from the `scikit-learn` Python package.

6.1 Convergence Analysis of Vendi Scores

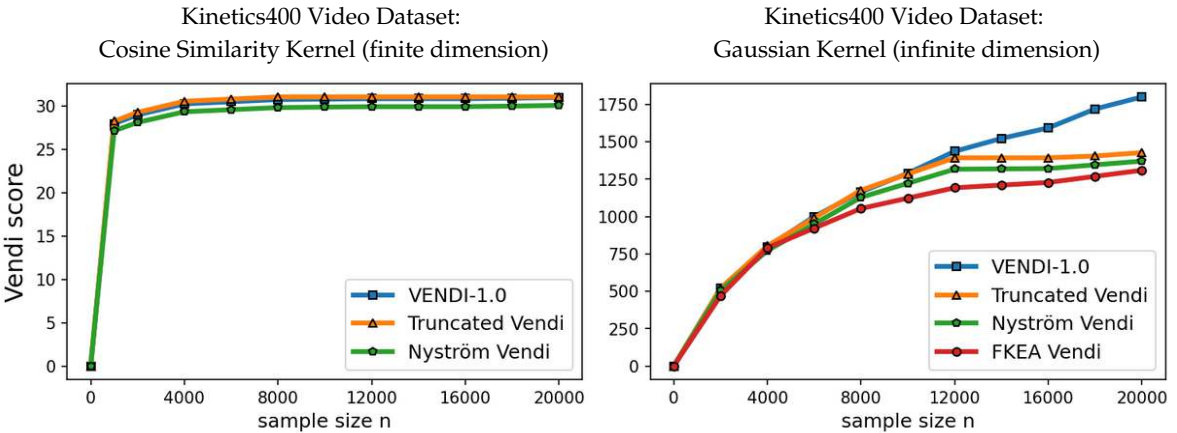
To assess the convergence of the discussed Vendi scores, we conducted experiments on four datasets including ImageNet and FFHQ [30] image datasets, a synthetic text dataset with 400k paragraphs generated by GPT-4 about 100 randomly selected countries, and the Kinetics video dataset [31]. Our results, presented in Figure 2, show that for the finite-dimension cosine similarity kernel the Vendi score converges rapidly to the underlying value and the proxy versions including truncated and Nyström Vendi scores were almost identical to the original Vendi score. This observation is consistent with our theoretical results on the convergence of Vendi scores under finite-dimension kernel maps. On the other hand, in the case of infinite dimension Gaussian kernel, we observed that the Vendi_1 score did not converge using 20k samples and the score value kept growing with a considerable rate. However, the t -truncated Vendi score with $t = 10000$ converged to its underlying statistic shortly after 10000 samples were used. Consistent with our theoretical result, the proxy Nyström and FKEA estimated scores with their rank hyperparameter matched with t also converged to the limit of the truncated Vendi scores. The numerical results show the connection between the truncated Vendi score and the existing kernel methods for approximating the Vendi score.



(a) Statistical convergence of Vendi score for different sample sizes on FFHQ[30] data: (Left plot) finite-dimension cosine similarity kernel (Right plot) infinite dimension Gaussian kernel with bandwidth $\sigma = 35$. *DINOv2* embedding (dimension 768) is used in computing the scores.



(b) Statistical convergence of Vendi score for different sample sizes on Synthetic Countries data: (Left plot) finite-dimension cosine similarity kernel (Right plot) infinite dimension Gaussian kernel with bandwidth $\sigma = 0.6$. *text-embedding-3-large* embedding (dimension 3072) is used in computing the scores.



(c) Statistical convergence of Vendi score for different sample sizes on Kinetics400[31] data: (Left plot) finite-dimension cosine similarity kernel (Right plot) infinite dimension Gaussian kernel with bandwidth $\sigma = 4.0$. *I3D* embedding (dimension 1024) is used in computing the scores.

Figure 2: Statistical convergence results for image, text and video data under finite and infinite dimensional kernel functions.

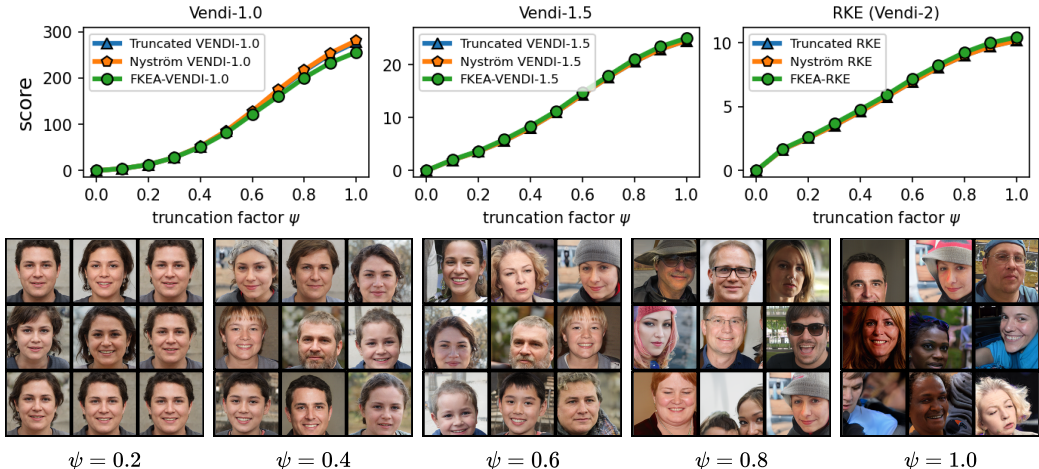


Figure 3: Diversity evaluation of Vendi scores on truncated StyleGAN3 generated FFHQ dataset with varying truncation coefficient ψ . Fixed sample size $n = 20k$ is used for estimating the scores.

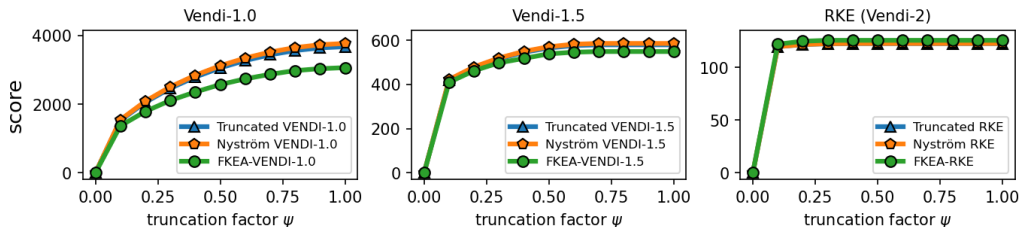


Figure 4: Diversity evaluation of Vendi scores on truncated StyleGAN-XL generated ImageNet dataset with varying truncation coefficient ψ . Fixed sample size $n = 20k$ is used for estimating the scores.

6.2 Correlation between the truncated Vendi score and diversity of data

We performed experiments to test the correlation between the truncated Vendi score and the ground-truth diversity of data. To do this, we applied the truncation technique to the FFHQ-based StyleGAN3 [32] model and the ImageNet-based StyleGAN-XL [33] model and simulated generative models with different underlying diversity by varying the truncation technique. Considering the Gaussian kernel, we estimated the t -truncated Vendi score with $t = 10000$ by averaging the estimated t -truncated Vendi scores over 5 independent datasets of size 20k where the score seemed to converge to its underlying value. Figures 3, 4 show how the estimated statistic correlates with the truncation parameter for order- α Vendi scores with $\alpha = 1, 1.5, 2$. In all these experiments, the estimated truncated Vendi score correlated with the underlying diversity of the models. In addition, we plot the proxy Nyström and FKEA proxy Vendi values computed using 20000 samples which remain close to the estimated t -truncated statistic. These empirical results suggest that the estimated t -truncated Vendi score with Gaussian kernel can be used to evaluate the diversity of generated data. Also, the Nyström and FKEA methods were both computationally efficient in estimating the truncated Vendi score from limited generated data. We defer the presentation of the additional numerical results on the convergence of Vendi scores with different orders, kernel functions and embedding spaces to the Appendix.

7 Conclusion

In this work, we investigated the statistical convergence behavior of Vendi diversity scores estimated from empirical samples. We highlighted that, due to the high computational complexity of the score for datasets larger than a few tens of thousands of generated data points, the score is often calculated using sample sizes below 10,000. We demonstrated that such restricted sample sizes do not pose a problem for statistical convergence as long as the kernel feature dimension is bounded. However, our numerical results showed a lack of convergence to the population Vendi when using an infinite-dimensional kernel map, such as the Gaussian kernel. To address this gap, we introduced the truncated population Vendi as an alternative target quantity for diversity evaluation. We showed that existing Nyström and FKEA methods for approximating Vendi scores concentrate around this truncated population Vendi. An interesting future direction is to explore the relationship between other kernel approximation techniques and the truncated population Vendi. Also, a comprehensive analysis of the computational-statistical trade-offs involved in estimating the Vendi score is another relevant future direction.

References

- [1] Dan Friedman and Adji Bousso Dieng. The vendi score: A diversity evaluation metric for machine learning. In *Transactions on Machine Learning Research*, 2023.
- [2] Mohammad Jalali, Cheuk Ting Li, and Farzan Farnia. An information-theoretic evaluation of generative models in learning multi-modal distributions. In *Advances in Neural Information Processing Systems*, volume 36, pages 9931–9943, 2023.
- [3] Jia Deng, Wei Dong, Richard Socher, Li-Jia Li, Kai Li, and Li Fei-Fei. Imagenet: A large-scale hierarchical image database. In *2009 IEEE conference on computer vision and pattern recognition (CVPR)*, pages 248–255. IEEE, 2009.
- [4] Tsung-Yi Lin, Michael Maire, Serge Belongie, James Hays, Pietro Perona, Deva Ramanan, Piotr Dollár, and C. Lawrence Zitnick. Microsoft COCO: Common objects in context. In David Fleet, Tomas Pajdla, Bernt Schiele, and Tinne Tuytelaars, editors, *European Conference on Computer Vision (ECCV)*, volume 8693, pages 740–755. Springer International Publishing, 2014. Book Title: Computer Vision – ECCV 2014 Series Title: Lecture Notes in Computer Science.
- [5] Maxime Oquab, Timothée Darcet, Théo Moutakanni, Huy V. Vo, Marc Szafraniec, Vasil Khalidov, Pierre Fernandez, Daniel Haziza, Francisco Massa, Alaaeldin El-Nouby, Mido Assran, Nicolas Ballas, Wojciech Galuba, Russell Howes, Po-Yao Huang, Shang-Wen Li, Ishan Misra, Michael Rabbat, Vasu Sharma, Gabriel Synnaeve, Hu Xu, Herve Jegou, Julien Mairal, Patrick Labatut, Armand Joulin, and Piotr Bojanowski. DINOv2: Learning robust visual features without supervision. In *Transactions on Machine Learning Research*, 2023.
- [6] Azim Ospanov, Jingwei Zhang, Mohammad Jalali, Xuenan Cao, Andrej Bogdanov, and Farzan Farnia. Towards a scalable reference-free evaluation of generative models. In *Advances in Neural Information Processing Systems*, volume 38, 2024.
- [7] Martin Heusel, Hubert Ramsauer, Thomas Unterthiner, Bernhard Nessler, and Sepp Hochreiter. GANs trained by a two time-scale update rule converge to a local nash equilibrium. In *Advances in Neural Information Processing Systems*, volume 30. Curran Associates, Inc., 2018.
- [8] Miłkołaj Bińkowski, Danica J Sutherland, Michael Arbel, and Arthur Gretton. Demystifying mmd gans. In *International Conference on Learning Representations*, 2018.
- [9] Mehdi S. M. Sajjadi, Olivier Bachem, Mario Lucic, Olivier Bousquet, and Sylvain Gelly. Assessing generative models via precision and recall. In *Advances in Neural Information Processing Systems*, volume 31. Curran Associates, Inc., 2018.

- [10] Tuomas Kynkäänniemi, Tero Karras, Samuli Laine, Jaakko Lehtinen, and Timo Aila. Improved precision and recall metric for assessing generative models. In *Advances in Neural Information Processing Systems*, volume 32. Curran Associates, Inc., 2019.
- [11] Muhammad Ferjad Naeem, Seong Joon Oh, Youngjung Uh, Yunjey Choi, and Jaejun Yoo. Reliable fidelity and diversity metrics for generative models. In *Proceedings of the 37th International Conference on Machine Learning*, volume 119 of *ICML'20*, pages 7176–7185. JMLR.org, 2020.
- [12] Krishna Pillutla, Swabha Swayamdipta, Rowan Zellers, John Thickstun, Sean Welleck, Yejin Choi, and Zaid Harchaoui. MAUVE: Measuring the gap between neural text and human text using divergence frontiers. In A. Beygelzimer, Y. Dauphin, P. Liang, and J. Wortman Vaughan, editors, *Advances in Neural Information Processing Systems*, 2021.
- [13] Krishna Pillutla, Lang Liu, John Thickstun, Sean Welleck, Swabha Swayamdipta, Rowan Zellers, Sewoong Oh, Yejin Choi, and Zaid Harchaoui. MAUVE Scores for Generative Models: Theory and Practice. *JMLR*, 2023.
- [14] Amey Pasarkar and Adji Bousso Dieng. Cousins of the vendi score: A family of similarity-based diversity metrics for science and machine learning. In *International Conference on Artificial Intelligence and Statistics*. PMLR, 2024.
- [15] J. Shawe-Taylor, C.K.I. Williams, N. Cristianini, and J. Kandola. On the eigenspectrum of the gram matrix and the generalization error of kernel-pca. *IEEE Transactions on Information Theory*, 51(7):2510–2522, 2005.
- [16] Francis Bach. Information Theory with Kernel Methods, August 2022. arXiv:2202.08545 [cs, math, stat].
- [17] Yuxin Dong, Tieliang Gong, Shujian Yu, and Chen Li. Optimal randomized approximations for matrix-based rényi’s entropy. *IEEE Transactions on Information Theory*, 2023.
- [18] Shai Fine and Katya Scheinberg. Efficient svm training using low-rank kernel representations. In *Journal of Machine Learning Research (JMLR)*, pages 243–250, 2001.
- [19] Francis R Bach and Michael I Jordan. Kernel independent component analysis. In *Journal of Machine Learning Research*, volume 3, pages 1–48, 2002.
- [20] Michael W. Mahoney and Petros Drineas. Cur matrix decompositions for improved data analysis. In *Proceedings of the National Academy of Sciences*, volume 106, pages 697–702, 2009.
- [21] Christopher Williams and Matthias Seeger. Using the nyström method to speed up kernel machines. In *Advances in neural information processing systems*, pages 682–688, 2000.
- [22] George Stein, Jesse Cresswell, Rasa Hosseinzadeh, Yi Sui, Brendan Ross, Valentin Vilecroze, Zhaoyan Liu, Anthony L Caterini, Eric Taylor, and Gabriel Loaiza-Ganem. Exposing flaws of generative model evaluation metrics and their unfair treatment of diffusion models. In A. Oh, T. Naumann, A. Globerson, K. Saenko, M. Hardt, and S. Levine, editors, *Advances in Neural Information Processing Systems*, volume 36, pages 3732–3784. Curran Associates, Inc., 2023.
- [23] Christian Szegedy, Vincent Vanhoucke, Sergey Ioffe, Jon Shlens, and Zbigniew Wojna. Rethinking the inception architecture for computer vision. In *2016 IEEE Conference on Computer Vision and Pattern Recognition (CVPR)*, 2016.
- [24] Alec Radford, Jong Wook Kim, Chris Hallacy, Aditya Ramesh, Gabriel Goh, Sandhini Agarwal, Girish Sastry, Amanda Askell, Pamela Mishkin, Jack Clark, Gretchen Krueger, and Ilya Sutskever. Learning Transferable Visual Models From Natural Language Supervision. In *International Conference on Machine Learning*, pages 8748–8763. arXiv, February 2021. arXiv:2103.00020 [cs].

- [25] Tuomas Kynkäänniemi, Tero Karras, Miika Aittala, Timo Aila, and Jaakko Lehtinen. The Role of ImageNet Classes in Fréchet Inception Distance. September 2022.
- [26] OpenAI. text-embedding-3-large. <https://platform.openai.com/docs/models/embeddings>, 2024.
- [27] João Carreira and Andrew Zisserman. Quo vadis, action recognition? a new model and the kinetics dataset. In *2017 IEEE Conference on Computer Vision and Pattern Recognition (CVPR)*, pages 4724–4733, 2017.
- [28] N. Aronszajn. Theory of reproducing kernels. *Transactions of the American Mathematical Society*, 68(3):337–404, 1950.
- [29] Alfréd Rényi. On measures of entropy and information. In *Proceedings of the Fourth Berkeley Symposium on Mathematical Statistics and Probability, Volume 1: Contributions to the Theory of Statistics*, pages 547–561. University of California Press, 1961.
- [30] Tero Karras, Samuli Laine, and Timo Aila. A style-based generator architecture for generative adversarial networks. In *Proceedings of the IEEE/CVF Conference on Computer Vision and Pattern Recognition (CVPR)*, pages 4401–4410, 2019.
- [31] Will Kay, Joao Carreira, Karen Simonyan, Brian Zhang, Chloe Hillier, Sudheendra Vijayanarasimhan, Fabio Viola, Tim Green, Trevor Back, Paul Natsev, Mustafa Suleyman, and Andrew Zisserman. The kinetics human action video dataset, 2017.
- [32] Tero Karras, Miika Aittala, Samuli Laine, Erik Härkönen, Janne Hellsten, Jaakko Lehtinen, and Timo Aila. Alias-free generative adversarial networks. In *Advances in Neural Information Processing Systems*, volume 34, pages 852–863. Curran Associates, Inc., 2021.
- [33] Axel Sauer, Katja Schwarz, and Andreas Geiger. Stylegan-xl: Scaling stylegan to large diverse datasets. In *ACM SIGGRAPH 2022 Conference Proceedings*, volume abs/2201.00273, 2022.
- [34] David Gross. Recovering low-rank matrices from few coefficients in any basis. *IEEE Transactions on Information Theory*, 57(3):1548–1566, 2011.
- [35] Jonas Moritz Kohler and Aurelien Lucchi. Sub-sampled cubic regularization for non-convex optimization. In *International Conference on Machine Learning*, pages 1895–1904. PMLR, 2017.
- [36] Zenglin Xu, Rong Jin, Bin Shen, and Shenghuo Zhu. Nystrom approximation for sparse kernel methods: Theoretical analysis and empirical evaluation. In *Proceedings of the AAAI Conference on Artificial Intelligence*, volume 29, 2015.
- [37] Mathilde Caron, Ishan Misra, Julien Mairal, Priya Goyal, Piotr Bojanowski, and Armand Joulin. Unsupervised Learning of Visual Features by Contrasting Cluster Assignments. In *Advances in Neural Information Processing Systems*, volume 33, pages 9912–9924. Curran Associates, Inc., 2020.

A Proofs

A.1 Proof of Theorem 1

To prove the theorem, we will use the following lemma followed from [34, 35].

Lemma 1 (Vector Bernstein Inequality [34, 35]). *Suppose that z_1, \dots, z_n are independent and identically distributed random vectors with zero mean $\mathbb{E}[z_i] = \mathbf{0}$ and bounded ℓ_2 -norm $\|z_i\|_2 \leq c$. Then, for every $0 \leq \epsilon \leq c$, the following holds*

$$\mathbb{P}\left(\left\|\frac{1}{n}\sum_{i=1}^n z_i\right\|_2 \geq \epsilon\right) \leq \exp\left(-\frac{n\epsilon^2}{8c^2} + \frac{1}{4}\right)$$

We apply the above Vector Bernstein Inequality to the random vectors $\phi(x_1) \otimes \phi(x_1), \dots, \phi(x_n) \otimes \phi(x_n)$ where \otimes denotes the Kronecker product. To do this, we define vector $v_i = \phi(x_i) \otimes \phi(x_i) - \mathbb{E}_{x \sim P}[\phi(x) \otimes \phi(x)]$ for every i . Note that v_i is, by definition, a zero-mean vector and also for every x we have the following for the normalized kernel function k :

$$\|\phi(x) \otimes \phi(x)\|_2^2 = \|\phi(x)\|_2^2 \cdot \|\phi(x)\|_2^2 = k(x, x) \cdot k(x, x) = 1$$

Then, the triangle inequality implies that

$$\|v_i\|_2 \leq \|\phi(x_i) \otimes \phi(x_i)\|_2 + \|\mathbb{E}_{x \sim P}[\phi(x) \otimes \phi(x)]\|_2 \leq \|\phi(x_i) \otimes \phi(x_i)\|_2 + \mathbb{E}_{x \sim P}[\|\phi(x) \otimes \phi(x)\|_2] = 2$$

As a result, the Vector Bernstein Inequality leads to the following for every $0 \leq \epsilon \leq 2$:

$$\mathbb{P}\left(\left\|\frac{1}{n}\sum_{i=1}^n \phi(x_i) \otimes \phi(x_i) - \mathbb{E}_{x \sim P}[\phi(x) \otimes \phi(x)]\right\|_2 \geq \epsilon\right) \leq \exp\left(\frac{8 - n\epsilon^2}{32}\right)$$

On the other hand, note that $\phi(x) \otimes \phi(x)$ is the vectorized version of rank-1 $\phi(x)\phi(x)^\top$, which shows that the above inequality is equivalent to the following where $\|\cdot\|_{\text{HS}}$ denotes the Hilbert-Schmidt norm, which will simplify to the Frobenius norm in the finite dimension case,

$$\begin{aligned} & \mathbb{P}\left(\left\|\frac{1}{n}\sum_{i=1}^n [\phi(x_i)\phi(x_i)^\top] - \mathbb{E}_{x \sim P}[\phi(x)\phi(x)^\top]\right\|_{\text{HS}} \geq \epsilon\right) \leq \exp\left(\frac{8 - n\epsilon^2}{32}\right) \\ \implies & \mathbb{P}\left(\|C_X - \tilde{C}_X\|_{\text{HS}} \geq \epsilon\right) \leq \exp\left(\frac{8 - n\epsilon^2}{32}\right) \end{aligned}$$

Subsequently, we can apply the Hoffman-Wielandt inequality which shows that for the sorted eigenvalue vectors of C_X (denoted by $\hat{\lambda}_n$ in the theorem) and \tilde{C}_X (denoted by $\tilde{\lambda}$ in the theorem) we will have $\|\hat{\lambda}_n - \tilde{\lambda}\|_2 \leq \|C_X - \tilde{C}_X\|_{\text{HS}}$, which together with the previous inequality leads to

$$\mathbb{P}\left(\|\hat{\lambda}_n - \tilde{\lambda}\|_2 \geq \epsilon\right) \leq \exp\left(\frac{8 - n\epsilon^2}{32}\right)$$

If we define $\delta = \exp((8 - n\epsilon^2)/32)$ that implies $\epsilon \leq \sqrt{\frac{32 \log(2/\delta)}{n}}$, we obtain the following for every $\delta \geq \exp((2 - n)/8)$ (since we suppose $0 \leq \epsilon \leq 2$)

$$\begin{aligned} & \mathbb{P}\left(\|\hat{\lambda}_n - \tilde{\lambda}\|_2 \geq \sqrt{\frac{32 \log(2/\delta)}{n}}\right) \leq \delta \\ \implies & \mathbb{P}\left(\|\hat{\lambda}_n - \tilde{\lambda}\|_2 \leq \sqrt{\frac{32 \log(2/\delta)}{n}}\right) \geq 1 - \delta \end{aligned}$$

which completes the proof.

A.2 Proof of Corollary 1

The case of $\alpha = 1$. We show that Theorem 1 on the concentration of the eigenvalues $\boldsymbol{\lambda} = [\lambda_1, \dots, \lambda_d]$ will further imply a concentration bound for the logarithm of Vendi-1 score. In the case of Vendi₁ (when $\alpha \rightarrow 1^+$), the concentration bound will be formed for the logarithm of the Vendi score, i.e. the Von-Neumann entropy (denoted as H_α):

$$H_1(C_X) := H_1(\boldsymbol{\lambda}) = \sum_{i=1}^d \tilde{\lambda}_i \log \frac{1}{\tilde{\lambda}_i}$$

Theorem 1 shows that $\|\widehat{\boldsymbol{\lambda}}_n - \tilde{\boldsymbol{\lambda}}\|_2 \leq \sqrt{\frac{32 \log(2/\delta)}{n}}$ with probability $1 - \delta$. To convert this concentration bound to a bound on the order-1 entropy (for Vendi-1 score) difference $H_1(\widehat{C}_n) - H_1(C_X)$, we leverage the following two lemmas:

Lemma 2. For every $0 \leq \alpha, \beta \leq 1$ such that $|\beta - \alpha| \leq \frac{1}{e}$, we have

$$\left| \alpha \log \frac{1}{\alpha} - \beta \log \frac{1}{\beta} \right| \leq |\beta - \alpha| \log \frac{1}{|\beta - \alpha|}$$

Proof. Let $c = |\alpha - \beta|$, where $c \in [0, \frac{1}{e}]$. Defining $g(z) = z \log(\frac{1}{z})$, the first-order optimality condition $g'(z) = -\log(z) - 1 = 0$ yields $\frac{1}{e}$ as the local maximum of $g(z)$. Therefore, there are three cases of placement of α and β on the interval $[0, 1]$: α and β appear before maximum point, after maximum point or maximum point is between α and β . We show that regardless of the placement of α and β , the above inequality remains true.

- **Case 1:** $\alpha, \beta \in [0, \frac{1}{e}]$. Note that $g''(z) = -\frac{1}{z^2}$. Since the second-order derivative is negative and the function g is monotonically increasing within the interval $[0, \frac{1}{e}]$, the gap between $g(\alpha)$ and $g(\beta)$ is maximized when $\alpha^* = 0$ and $\beta^* = c - \alpha^* = c$. This directly leads to the desired bound as follows:

$$\left| \alpha \log \frac{1}{\alpha} - \beta \log \frac{1}{\beta} \right| \leq \left| \alpha^* \log \frac{1}{\alpha^*} - \beta^* \log \frac{1}{\beta^*} \right| = |0 \log 0 - c \log \frac{1}{c}| \leq c \log \frac{1}{c}$$

Here, we use the standard limit $0 \log 0 = 0$.

- **Case 2:** $\alpha, \beta \in [\frac{1}{e}, 1]$. In this case, we note that g is concave yet decreasing over $[\frac{1}{e}, 1]$, and so the gap between $g(\alpha)$ and $g(\beta)$ will be maximized when $\alpha^* = 1 - c$ and $\beta^* = 1$. This leads to:

$$\left| \alpha \log \frac{1}{\alpha} - \beta \log \frac{1}{\beta} \right| \leq \left| \alpha^* \log \frac{1}{\alpha^*} - \beta^* \log \frac{1}{\beta^*} \right| = (1 - c) \log \frac{1}{(1 - c)} \leq c \log \frac{1}{c}$$

where the last inequality holds because $c \in [0, \frac{1}{e}]$, and if we define the function $h(c) = c \log \frac{1}{c} - (1 - c) \log \frac{1}{1 - c}$, then we have $h'(c) = \log \frac{1}{c(1 - c)} - 2$, which is positive over $c \in [0, c_0]$ ($e^{-2} < c_0 < e^{-1}$ is where $c_0(1 - c_0) = e^{-2}$), and then negative over $[c_0, \frac{1}{e}]$, and hence $h(c) \geq \min\{h(0), h(1/e)\} = 0$ for every $c \in [0, 1/e]$.

- **Case 3:** $\alpha \in [0, \frac{1}{e}]$ and $\beta \in (\frac{1}{e}, 1]$. When α and β lie on the opposite ends from the maximum point, the inequality becomes:

$$\left| \alpha \log \frac{1}{\alpha} - \beta \log \frac{1}{\beta} \right| \leq \max \left\{ \left| (1/e) \log \frac{1}{1/e} - \beta \log \frac{1}{\beta} \right|, \left| \alpha \log \frac{1}{\alpha} - (1/e) \log \frac{1}{1/e} \right| \right\} \leq c \log \frac{1}{c}$$

since we pick the side with the largest difference, this difference is upper bounded by either Case 1 or Case 2 because $\max\{|\frac{1}{e} - \beta|, |\alpha - \frac{1}{e}|\} < c$. Therefore, this case is upper-bounded by $c \log \frac{1}{c}$.

All the three cases of placement of α and β are upper-bounded by $c \log \frac{1}{c}$; Therefore, the claim holds. \square

Lemma 3. If $\|\mathbf{u}\|_2 \leq \epsilon$ for d -dimensional vector $\mathbf{u} \geq \mathbf{0}$ where $\epsilon \leq \frac{1}{e}$, then we have

$$\sum_{i=1}^d u_i \log \frac{1}{u_i} \leq \epsilon \sqrt{d} \log \frac{\sqrt{d}}{\epsilon}$$

Proof. We prove the above inequality using the KKT conditions for the following maximization problem, representing a convex optimization problem,

$$\begin{aligned} \max_{\mathbf{u} \in \mathbb{R}^d} \quad & \sum_{i=1}^d u_i \log\left(\frac{1}{u_i}\right) \\ \text{subject to} \quad & u_i \geq 0, \text{ for all } i \\ & \sum_{i=1}^d u_i^2 \leq \epsilon^2 \quad (\text{equivalent to } \|\mathbf{u}\|_2 \leq \epsilon) \end{aligned}$$

In a concave maximization problem subject to convex constraints, any point that satisfies the KKT conditions is guaranteed to be a global optimum. Let us pick the following solution $\mathbf{u}^* = \frac{\epsilon}{\sqrt{d}} \mathbf{1}$ and slack variables $\lambda^* = \frac{\sqrt{d}}{2\epsilon} (\log(\frac{\sqrt{d}}{\epsilon}) - 1)$, $\forall_i \mu_i^* = 0$. The Lagrangian of the above problem:

$$L(\mathbf{u}, \lambda, \mu_1, \dots, \mu_d) = \sum_{i=1}^d u_i \log\left(\frac{1}{u_i}\right) + \lambda(\epsilon^2 - \sum_{i=1}^d u_i^2) - \sum_{i=1}^d \mu_i u_i$$

- **Primal Feasibility.** The solution \mathbf{u}^* satisfies the primal feasibility, since $\epsilon^2 - \sum_{i=1}^d (\frac{\epsilon}{\sqrt{d}})^2 = \epsilon^2 - d \frac{\epsilon^2}{d} = 0$ and $\frac{\epsilon}{\sqrt{d}} \geq 0$.
- **Dual Feasibility.** $\lambda^* \geq 0$ is feasible because of the assumption $\epsilon \leq \frac{1}{e}$ implying that $\frac{\sqrt{d}}{\epsilon} \geq e$ for every integer dimension $d \geq 1$. Note that this implies $\lambda^* = \frac{\sqrt{d}}{2\epsilon} (\log(\frac{\sqrt{d}}{\epsilon}) - 1) \geq 0$.
- **Complementary Slackness.** Since $\lambda^*(\epsilon^2 - \sum_{i=1}^d (\frac{\epsilon}{\sqrt{d}})^2) = \lambda^* \cdot 0 = 0$, the condition is satisfied.
- **Stationarity.** The condition is satisfied as follows:

$$\frac{\partial}{\partial u_i} L(\mathbf{u}^*) = -\log(u_i^*) - 1 - 2\lambda^* u_i^* + \mu_i^* = -\log\left(\frac{\epsilon}{\sqrt{d}}\right) - 1 - 2 \cdot \frac{\sqrt{d}}{2\epsilon} \left(-\log\left(\frac{\epsilon}{\sqrt{d}}\right) - 1\right) \cdot \frac{\epsilon}{\sqrt{d}} = 0$$

Since all KKT conditions are satisfied and sufficient for global optimality, $\mathbf{u}^* = \frac{\epsilon}{\sqrt{d}} \mathbf{1}$ is a global optimum of the specified concave maximization problem. We note that this result is also implied by the Schur-concavity property of entropy. Following this result, the specified objective is upper-bounded as follows:

$$\sum_{i=1}^d u_i \log \frac{1}{u_i} \leq \epsilon \sqrt{d} \log \frac{\sqrt{d}}{\epsilon}$$

Therefore, the lemma's proof is complete. □

Following the above lemmas, knowing that $\|\hat{\lambda}_n - \tilde{\lambda}\|_2 \leq \sqrt{\frac{32 \log(2/\delta)}{n}}$ from Theorem 1 and using the assumption $n \geq 32e^2 \log(2/\delta) \approx 236.5 \log(2/\delta)$ that ensures the upper-bound satisfies $\sqrt{\frac{32 \log(2/\delta)}{n}} \leq \frac{1}{e}$, we can apply the above two lemmas to show that with probability $1 - \delta$:

$$\left| H_1(\widehat{C}_n) - H_1(C_X) \right| = \left| H_1(\widehat{\lambda}_n) - H_1(\widetilde{\lambda}) \right| \leq \sqrt{\frac{8d \log(2/\delta)}{n}} \log\left(\frac{nd}{32 \log(2/\delta)}\right)$$

Note that under a kernel function with finite dimension d , the above bound will be $\mathcal{O}\left(\sqrt{\frac{d}{n}} \log(nd)\right)$.

The case of $1 < \alpha < 2$. Note that the inequality $\|v\|_\alpha \leq d^{\frac{2-\alpha}{2}} \|v\|_2$ holds for every d -dimensional vector $v \in \mathbb{R}^d$. Therefore, we can repeat the proof of Corollary 2 to show the following for every $1 < \alpha < 2$

$$\begin{aligned} \left| \text{Vendi}_\alpha(x_1, \dots, x_n)^{\frac{1-\alpha}{\alpha}} - \text{Vendi}_\alpha(P_x)^{\frac{1-\alpha}{\alpha}} \right| &= \left| \|\widehat{\lambda}_n\|_\alpha - \|\widetilde{\lambda}\|_\alpha \right| \\ &\leq \|\widehat{\lambda}_n - \widetilde{\lambda}\|_\alpha \\ &\leq d^{\frac{2-\alpha}{2}} \|\widehat{\lambda}_n - \widetilde{\lambda}\|_2. \end{aligned}$$

Consequently, Theorem 1 implies that for every $1 \leq \alpha < 2$ and $\delta \geq \exp((2-n)/8)$, the following holds with probability at least $1 - \delta$

$$\left| \text{Vendi}_\alpha(x_1, \dots, x_n)^{\frac{1-\alpha}{\alpha}} - \text{Vendi}_\alpha(P_x)^{\frac{1-\alpha}{\alpha}} \right| \leq d^{\frac{2-\alpha}{2}} \sqrt{\frac{32 \log(2/\delta)}{n}} = \sqrt{\frac{32d^{2-\alpha} \log(2/\delta)}{n}}$$

A.3 Proof of Corollary 2

Considering the α -norm definition $\|\mathbf{v}\|_\alpha = (\sum_{i=1}^d |v_i|^\alpha)^{1/\alpha}$, we can rewrite the order- α Vendi definition as

$$\text{Vendi}_\alpha(x_1, \dots, x_n) = \|\widehat{\lambda}_n\|_\alpha^{\frac{\alpha}{1-\alpha}} \iff \text{Vendi}_\alpha(x_1, \dots, x_n)^{\frac{1-\alpha}{\alpha}} = \|\widehat{\lambda}_n\|_\alpha$$

where $\widehat{\lambda}_n$ is defined in Theorem 1. Similarly, given the definition of $\widetilde{\lambda}$ we can write

$$\text{Vendi}_\alpha(P_x)^{\frac{1-\alpha}{\alpha}} = \|\widetilde{\lambda}\|_\alpha$$

Therefore, for every $\alpha \geq 2$, the following hold due to the triangle inequality:

$$\begin{aligned} \left| \text{Vendi}_\alpha(x_1, \dots, x_n)^{\frac{1-\alpha}{\alpha}} - \text{Vendi}_\alpha(P_x)^{\frac{1-\alpha}{\alpha}} \right| &= \left| \|\widehat{\lambda}_n\|_\alpha - \|\widetilde{\lambda}\|_\alpha \right| \\ &\leq \|\widehat{\lambda}_n - \widetilde{\lambda}\|_\alpha \\ &\leq \|\widehat{\lambda}_n - \widetilde{\lambda}\|_2. \end{aligned}$$

As a result, Theorem 1 shows that for every $\alpha \geq 2$ and $\delta \geq \exp((2-n)/8)$, the following holds with probability at least $1 - \delta$

$$\left| \text{Vendi}_\alpha(x_1, \dots, x_n)^{\frac{1-\alpha}{\alpha}} - \text{Vendi}_\alpha(P_x)^{\frac{1-\alpha}{\alpha}} \right| \leq \sqrt{\frac{32 \log(2/\delta)}{n}}$$

A.4 Proof of Theorem 2

We begin by proving the following lemma showing that the eigenvalues used in the definition of the t -truncated Vendi score are the projection of the original eigenvalues onto a t -dimensional probability simplex.

Lemma 4. Consider $\mathbf{v} \in [0, 1]^d$ that satisfies $\mathbf{1}^\top \mathbf{v} = 1$. i.e., the sum of \mathbf{v} 's entries equals 1. Given integer $1 \leq t \leq d$, define vector $\mathbf{v}^{(t)} \in [0, 1]^d$ whose last $d - t$ entries are 0, i.e., $v_i^{(t)} = 0$ for $t + 1 \leq i \leq d$, and its first t entries are defined as $v_j^{(t)} = v_j + \frac{1 - S_t}{t}$ where $S_t = v_1 + \dots + v_t$. Then, $\mathbf{v}^{(t)}$ is the projection of \mathbf{v} onto the following simplex set and has the minimum ℓ_2 -norm distance to this set

$$\Delta_t := \left\{ \mathbf{u} \in [0, 1]^d : v_i = 0 \text{ for all } t + 1 \leq i \leq d, \sum_{i=1}^t v_i = 1 \right\}.$$

Proof. To prove the lemma, first note that $\mathbf{v}^{(t)} \in \Delta_t$, i.e. its first t entries are non-negative and add up to 1, and also its last $d - t$ entries are zero. Then, consider the projection problem discussed in the lemma:

$$\begin{aligned} \min_{\mathbf{u} \in \mathbb{R}^t} \quad & \sum_{i=1}^t (u_i - v_i)^2 \\ \text{subject to} \quad & u_i \geq 0, \text{ for all } i \\ & \sum_{i=1}^t u_i = 1 \end{aligned}$$

Then, since we know from the assumptions that $v_i \geq 0$ and $\sum_{i=1}^t v_i \leq 1$, the discussed $\mathbf{u}^* \in \mathbb{R}^t$ where $u_i^* = v_i + (1 - S_t)/t$ together with Lagrangian coefficients $\mu_i = 0$ (for inequality constraint $u_i \geq 0$) and $\lambda = (1 - S_t)/t$ (for equality constraint) satisfy the KKT conditions. The primal and dual feasibility conditions as well as the complementary slackness clearly hold for these selection of primal and dual variables. Also, the KKT stationarity condition is satisfied as for every i we have $u_i^* - v_i - \lambda - \mu_i = 0$. Since the optimization problem is a convex optimization task with affine constraints, the KKT conditions are sufficient for optimality which proves the lemma. \square

Based on the above lemma, the eigenvalues $\widehat{\lambda}_n^{(t)}$ used to calculate the t -truncated Vendi score $\text{Vendi}_\alpha^{(t)}(x_1, \dots, x_n)$ are the projections of the top- t eigenvalues in $\widehat{\lambda}_n$ for the original score $\text{Vendi}_\alpha(x_1, \dots, x_n)$ onto the t -simplex subset of \mathbb{R}^d according to the ℓ_2 -norm. Similarly, the eigenvalues $\widetilde{\lambda}_n^{(t)}$ used to calculate the t -truncated population Vendi $\text{Vendi}_\alpha^{(t)}(P_X)$ are the projections of the top- t eigenvalues in $\widetilde{\lambda}$ for the original population Vendi $\text{Vendi}_\alpha(P_x)$ onto the t -simplex subset of \mathbb{R}^d .

Since ℓ_2 -norm is a Hilbert space norm and the t -simplex subset Δ_t is a convex set, we know from the convex analysis that the ℓ_2 -distance between the projected points $\widehat{\lambda}_n^{(t)}$ and $\widetilde{\lambda}^{(t)}$ is upper-bounded by the ℓ_2 -distance between the original points $\widehat{\lambda}_n$ and $\widetilde{\lambda}$. As a result, Theorem 1 implies that

$$\begin{aligned} \mathbb{P}\left(\|\widehat{\lambda}_n - \widetilde{\lambda}\|_2 \leq \sqrt{\frac{32 \log(2/\delta)}{n}}\right) &\geq 1 - \delta \\ \implies \mathbb{P}\left(\|\widehat{\lambda}_n^{(t)} - \widetilde{\lambda}^{(t)}\|_2 \leq \sqrt{\frac{32 \log(2/\delta)}{n}}\right) &\geq 1 - \delta \end{aligned}$$

However, note that the eigenvalue vectors $\widehat{\lambda}_n^{(t)}$ and $\widetilde{\lambda}^{(t)}$ can be analyzed in a bounded t -dimensional space as their entries after index $t + 1$ are zero. Therefore, we can apply the proof of Corollary 1 to show that for every $1 \leq \alpha < 2$ and $\delta \geq \exp((2 - n)/8)$, the following holds with probability at least $1 - \delta$

$$\left| \text{Vendi}_\alpha(x_1, \dots, x_n)^{\frac{1-\alpha}{\alpha}} - \text{Vendi}_\alpha(P_x)^{\frac{1-\alpha}{\alpha}} \right| \leq \sqrt{\frac{32 t^{2-\alpha} \log(2/\delta)}{n}}$$

To extend the result to a general $\alpha > 1$, we reach the following inequality covering the above result as well as the result of Corollary 2 in one inequality

$$\left| \text{Vendi}_\alpha(x_1, \dots, x_n)^{\frac{1-\alpha}{\alpha}} - \text{Vendi}_\alpha(P_x)^{\frac{1-\alpha}{\alpha}} \right| \leq \sqrt{\frac{32 \max\{1, t^{2-\alpha}\} \log(2/\delta)}{n}}$$

A.5 Proof of Theorem 3

Proof of Part (a). As defined by [6], the FKEA method uses the eigenvalues of t random Fourier frequencies $\omega_1, \dots, \omega_t$ where for each ω_i they consider two features $\cos(\omega_i^\top x)$ and $\sin(\omega_i^\top x)$. Following the definitions, it can be seen that $k(x, x') = \mathbb{E}_{\omega \sim p_\omega} [\cos(\omega^\top (x - x'))]$ which is approximated by FKEA

as $\frac{1}{t} \sum_{i=1}^t \cos(\omega_i^\top (x - x'))$. Therefore, if we define kernel matrix K_i as the kernel matrix for $k_i(x, x') = \cos(\omega_i^\top (x - x'))$, then we will have

$$\frac{1}{n} K^{\text{FKEA}(t)} = \frac{1}{t} \sum_{i=1}^t \frac{1}{n} K_i$$

where $\mathbb{E}_{\omega_i \sim p_\omega} [\frac{1}{n} K_i] = \frac{1}{n} K$.

On the other hand, we note that $\|\frac{1}{n} K\|_{\text{HS}} \leq 1$ holds as the kernel function is normalized and hence $|k(x, x')| \leq 1$. Since the Frobenius norm is the ℓ_2 -norm of the vectorized version of the matrix, we can apply Vector Bernstein inequality in Lemma 1 to show that for every $0 \leq \epsilon \leq 2$:

$$\begin{aligned} \mathbb{P}\left(\left\|\frac{1}{t} \sum_{i=1}^t \left[\frac{1}{n} K_i\right] - \frac{1}{n} K\right\|_F \geq \epsilon\right) &\leq \exp\left(\frac{8 - t\epsilon^2}{32}\right) \\ \implies \mathbb{P}\left(\left\|\frac{1}{n} K^{\text{FKEA}(t)} - \frac{1}{n} K\right\|_F \geq \epsilon\right) &\leq \exp\left(\frac{8 - t\epsilon^2}{32}\right) \end{aligned}$$

Then, we apply the Hoffman-Wielandt inequality to show that for the sorted eigenvalue vectors of $\frac{1}{n} K$ (denoted by $\widehat{\lambda}_n$) and $\frac{1}{n} K^{\text{FKEA}(t)}$ (denoted by $\lambda^{\text{FKEA}(t)}$) we will have $\|\widehat{\lambda}_n - \lambda^{\text{FKEA}(t)}\|_2 \leq \|\frac{1}{n} K^{\text{FKEA}(t)} - \frac{1}{n} K\|_{\text{HS}}$, which together with the previous inequality leads to

$$\mathbb{P}\left(\|\widehat{\lambda}_n - \lambda^{\text{FKEA}(t)}\|_2 \geq \epsilon\right) \leq \exp\left(\frac{8 - t\epsilon^2}{32}\right)$$

Furthermore, as we shown in the proof of Theorem 1 for every $0 \leq \gamma \leq 2$

$$\mathbb{P}\left(\|\widehat{\lambda}_n - \widetilde{\lambda}\|_2 \geq \gamma\right) \leq \exp\left(\frac{8 - n\gamma^2}{32}\right)$$

which, by applying the union bound for $\gamma = \epsilon$, together with the previous inequality shows that

$$\begin{aligned} \mathbb{P}\left(\|\widetilde{\lambda} - \lambda^{\text{FKEA}(t)}\|_2 \geq 2\epsilon\right) &\leq \exp\left(\frac{8 - t\epsilon^2}{32}\right) + \exp\left(\frac{8 - n\epsilon^2}{32}\right) \\ &\leq 2 \exp\left(\frac{8 - \min\{n, t\}\epsilon^2}{32}\right) \end{aligned}$$

Therefore, Lemma 4 implies that

$$\mathbb{P}\left(\|\widetilde{\lambda}^{(t)} - \lambda^{\text{FKEA}(t)}\|_2 \geq \epsilon\right) \leq 2 \exp\left(\frac{32 - \min\{n, t\}\epsilon^2}{128}\right)$$

If we define $\delta = 2 \exp\left(\frac{32 - \min\{n, t\}\epsilon^2}{128}\right)$, implying that $\epsilon \leq \sqrt{\frac{128 \log(3/\delta)}{\min\{n, t\}}}$, then the above inequality shows that

$$\mathbb{P}\left(\|\widetilde{\lambda}^{(t)} - \lambda^{\text{FKEA}(t)}\|_2 \leq \sqrt{\frac{128 \log(3/\delta)}{\min\{n, t\}}}\right) \geq 1 - \delta$$

Therefore, if we follow the same steps of the proof of Theorem 2, we can show

$$\left| \text{FKEA-Vendi}_\alpha^{(t)}(x_1, \dots, x_n)^{\frac{1-\alpha}{\alpha}} - \text{Vendi}_\alpha^{(t)}(P_x)^{\frac{1-\alpha}{\alpha}} \right| \leq \sqrt{\frac{128 \max\{1, t^{2-\alpha}\} \log(3/\delta)}{\min\{n, t\}}}$$

Proof of Part (b). To show this theorem, we use Theorem 3 from [36], which shows that if the r th largest eigenvalue of the kernel matrix $\frac{1}{n} K$ satisfies $\lambda_r \leq \frac{\tau}{n}$, then given $t \geq Cr \log(n)$ (C is a universal constant), the following spectral norm bound will hold with probability $1 - \frac{2}{n^3}$:

$$\left\| \frac{1}{n} K - \frac{1}{n} K^{\text{Nystrom}(t)} \right\|_{sp} \leq \mathcal{O}\left(\frac{\tau \log(n)}{\sqrt{nt}}\right).$$

Therefore, Weyl's inequality implies the following for the vector of sorted eigenvalues of $\frac{1}{n}K$, i.e. $\widehat{\lambda}_n$, and that of $\frac{1}{n}K^{\text{Nystrom}(t)}$, i.e., $\lambda^{\text{Nystrom}(t)}$,

$$\|\widehat{\lambda}_n - \lambda^{\text{Nystrom}(t)}\|_\infty \leq \mathcal{O}\left(\frac{\tau \log(n)}{\sqrt{nt}}\right).$$

As a result, considering the subvectors $\widehat{\lambda}_n[1:t]$ and $\lambda^{\text{Nystrom}(t)}[1:t]$ with the first t entries of the vectors, we will have:

$$\|\widehat{\lambda}_n[1:t] - \lambda^{\text{Nystrom}(t)}[1:t]\|_\infty \leq \mathcal{O}\left(\frac{\tau \log(n)}{\sqrt{nt}}\right) \implies \|\widehat{\lambda}_n[1:t] - \lambda^{\text{Nystrom}(t)}[1:t]\|_2 \leq \mathcal{O}\left(\tau \log(n) \sqrt{\frac{t}{n}}\right)$$

Noting that the non-zero entries of $\lambda^{\text{Nystrom}(t)}$ are all included in the first- t elements, we can apply Lemma 4 which shows that with probability $1 - 2n^{-3}$ we have

$$\|\widehat{\lambda}_n^{(t)} - \lambda^{\text{Nystrom}(t)}\|_2 \leq \mathcal{O}\left(\tau \log(n) \sqrt{\frac{t}{n}}\right)$$

Also, in the proof of Theorem 2, we showed that

$$\mathbb{P}\left(\|\widehat{\lambda}_n^{(t)} - \widetilde{\lambda}^{(t)}\|_2 \leq \sqrt{\frac{32 \log(2/\delta)}{n}}\right) \geq 1 - \delta$$

Combining the above inequalities using a union bound, shows that with probability at least $1 - \delta - 2n^{-3}$ we have

$$\begin{aligned} \|\lambda^{\text{Nystrom}(t)} - \widetilde{\lambda}^{(t)}\|_2 &\leq \|\lambda^{\text{Nystrom}(t)} - \widehat{\lambda}_n^{(t)}\|_2 + \|\widehat{\lambda}_n^{(t)} - \widetilde{\lambda}^{(t)}\|_2 \\ &\leq \sqrt{\frac{32 \log(2/\delta)}{n}} + \mathcal{O}\left(\tau \log(n) \sqrt{\frac{t}{n}}\right) \\ &= \mathcal{O}\left(\sqrt{\frac{\log(2/\delta) + t \log(n)^2 \tau^2}{n}}\right) \end{aligned}$$

Hence, repeating the final steps in the proof of Theorem 2, we can prove

$$\left| \text{Nystrom-Vendi}_\alpha^{(t)}(x_1, \dots, x_n)^{\frac{1-\alpha}{\alpha}} - \text{Vendi}_\alpha^{(t)}(P_x)^{\frac{1-\alpha}{\alpha}} \right| \leq \mathcal{O}\left(\sqrt{\frac{\max\{t^{2-\alpha}, 1\} (\log(2/\delta) + t \log(n)^2 \tau^2)}{n}}\right)$$

B Additional Numerical Results

In this section, we present supplementary results concerning the evaluation of diversity and the convergence behavior of different variants of the Vendi score. We extend the convergence experiments discussed in the main text to include the truncated StyleGAN3-t FFHQ dataset (Figure 9) and the StyleGAN-XL ImageNet dataset (Figure 10). Furthermore, we demonstrate that the truncated Vendi statistic effectively captures the diversity characteristics across various data modalities. Specifically, we conducted similar experiments as shown in Figures 4 and 3 on text data (Figure 6) and video data (Figure 8), showcasing the applicability of the metric across different domains.

We observe in Figure 9 that the convergence behavior is illustrated across various values of ψ . The results indicate that, for a fixed bandwidth σ , the truncated, Nyström, and FKEA variants of the Vendi score converge to the truncated Vendi statistic. As demonstrated in Figure 3 of the main text, this truncated Vendi statistic effectively captures the diversity characteristics inherent in the underlying dataset.

We note that in presence of incremental changes to the diversity of the dataset, finite-dimensional kernels, such as cosine similarity kernel, remain relatively constant. This effect is illustrated in Figure 10, where increase in truncation factor ψ results in incremental change in diversity. This is one of the cases where infinite-dimensional kernel maps with a sensitivity (bandwidth) parameter σ are useful in controlling how responsive the method should be to the change in diversity.

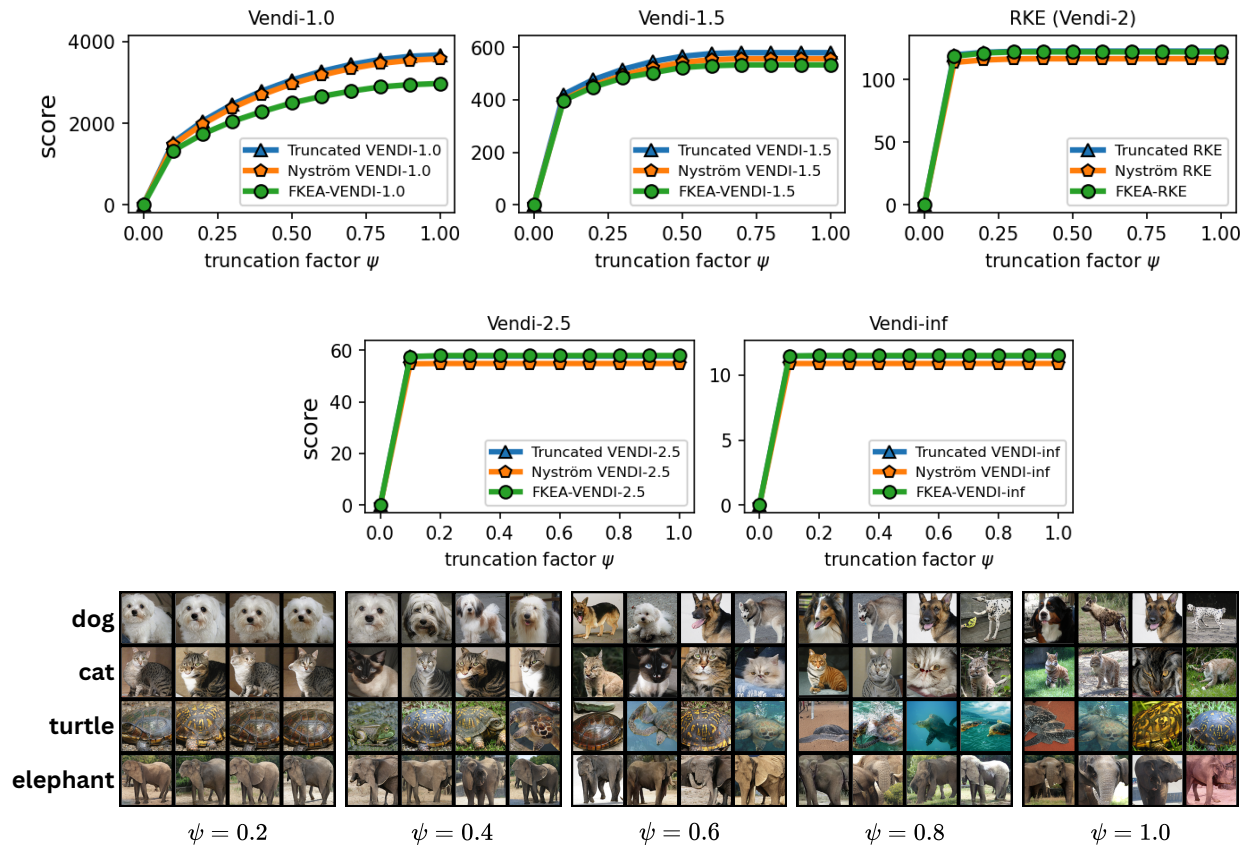


Figure 5: Diversity evaluation of Vendi scores on StyleGAN-XL generated ImageNet dataset with varying truncation parameter ψ . The setting is based on *Dino V2* embedding and bandwidth $\sigma = 30$

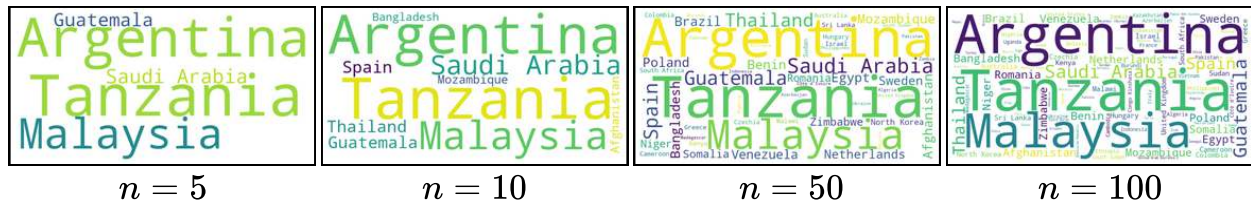
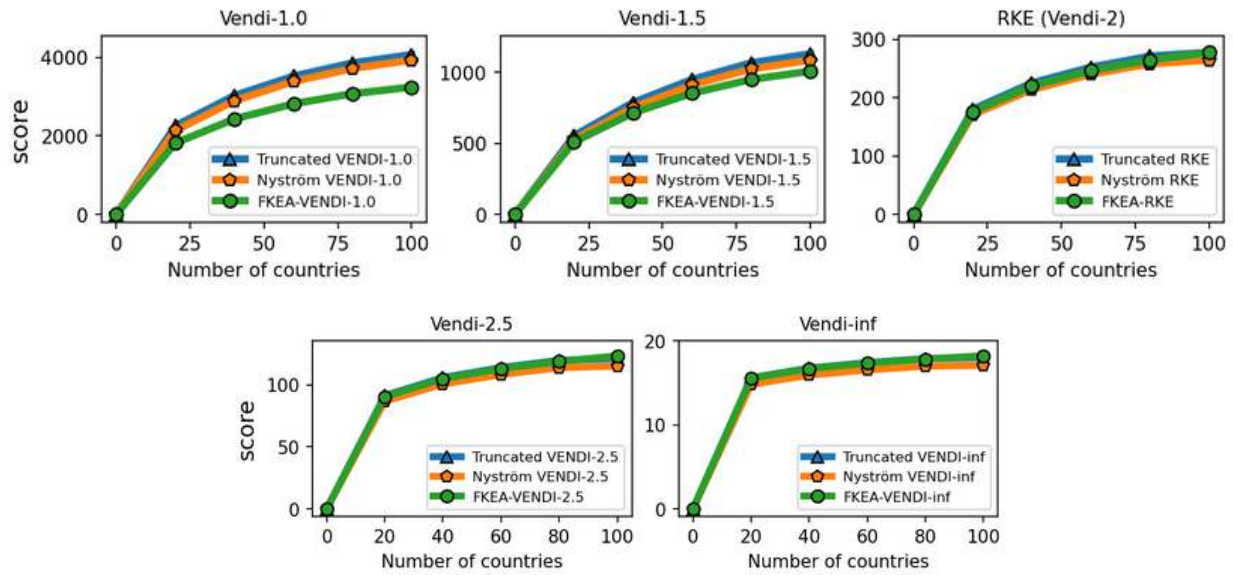


Figure 6: Diversity evaluation of Vendi scores on synthetic text dataset about 100 countries generated by GPT-4 with varying number of countries. The setting is based on *text-embedding-3-large* embedding and bandwidth $\sigma = 0.5$

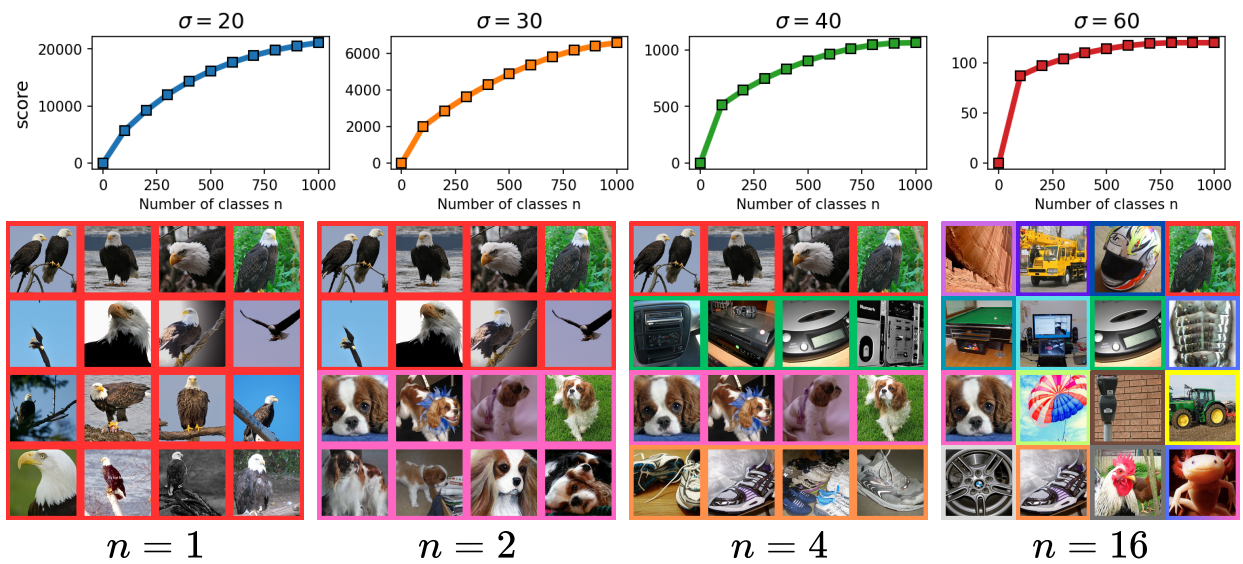


Figure 7: The diagram outlining an intuition behind a kernel bandwidth σ selection in diversity evaluation.

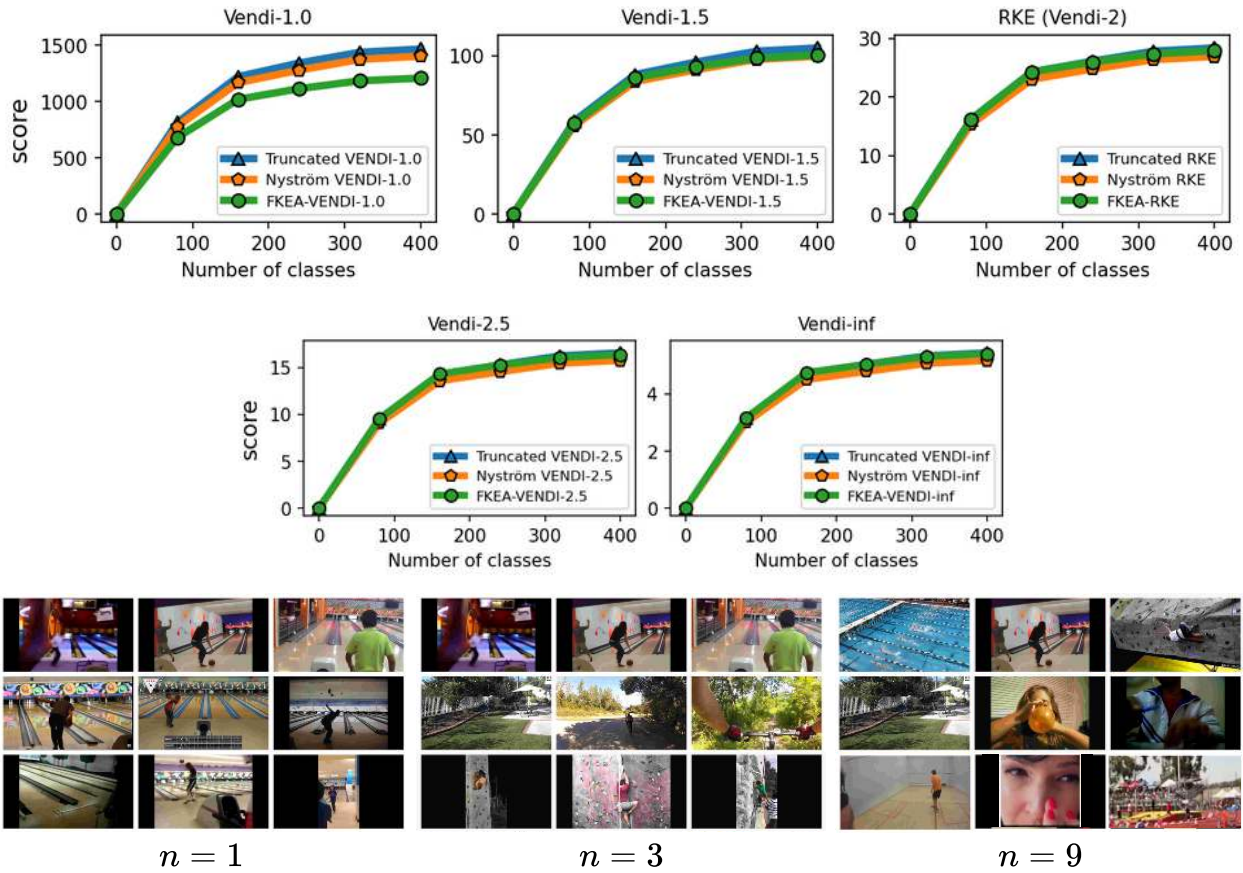


Figure 8: Diversity evaluation of Vendi scores on Kinetics400 dataset with varying number of classes. The setting is based on $I3D$ embedding and bandwidth $\sigma = 4.0$

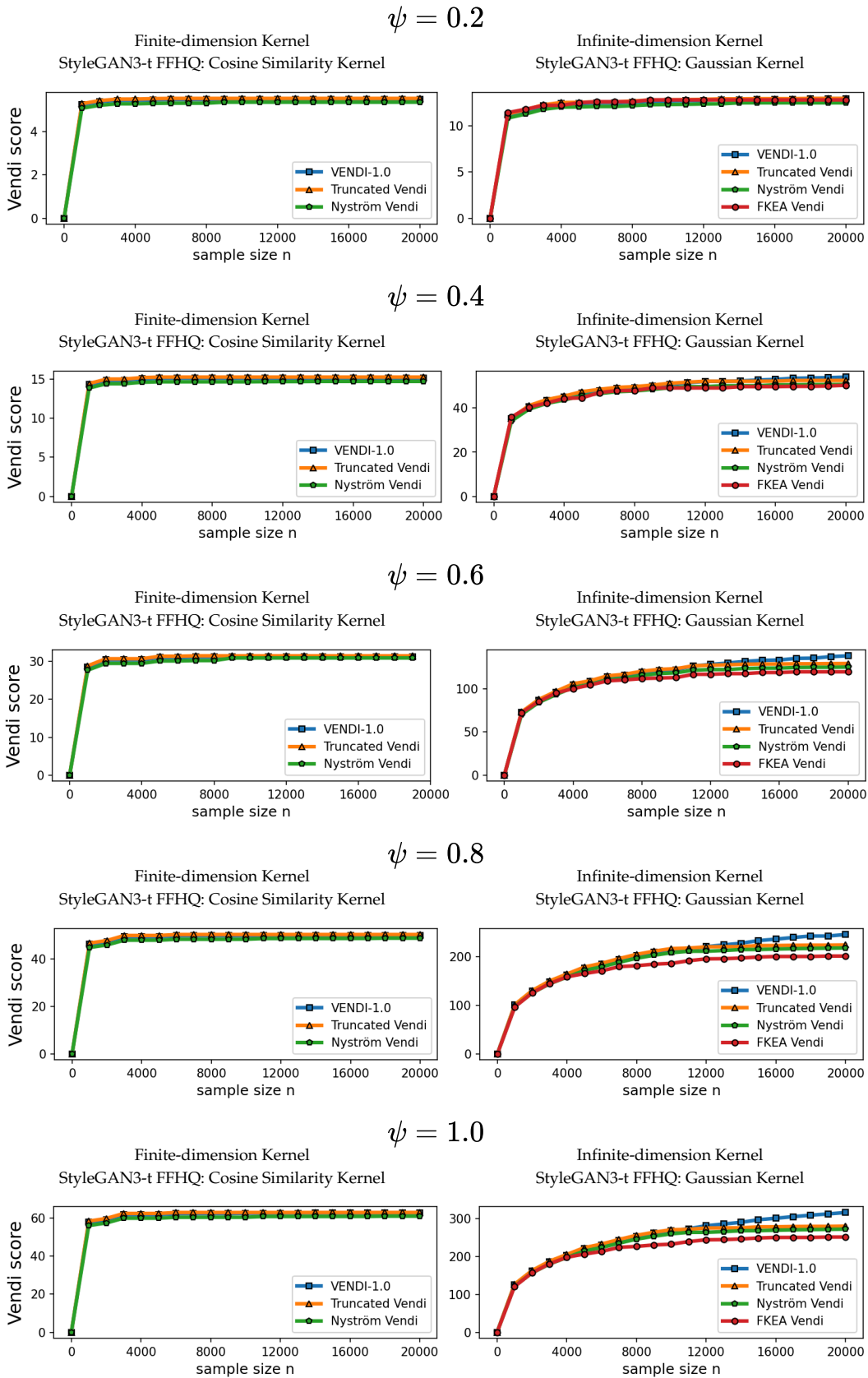


Figure 9: Statistical convergence of Vendi score for different sample sizes on StyleGAN3 generated FFHQ data at various truncation factors ψ : (Left plot) finite-dimension cosine similarity kernel (Right plot) infinite dimension Gaussian kernel with bandwidth $\sigma = 35$. *DinoV2* embedding (dimension 768) is used in computing the scores.

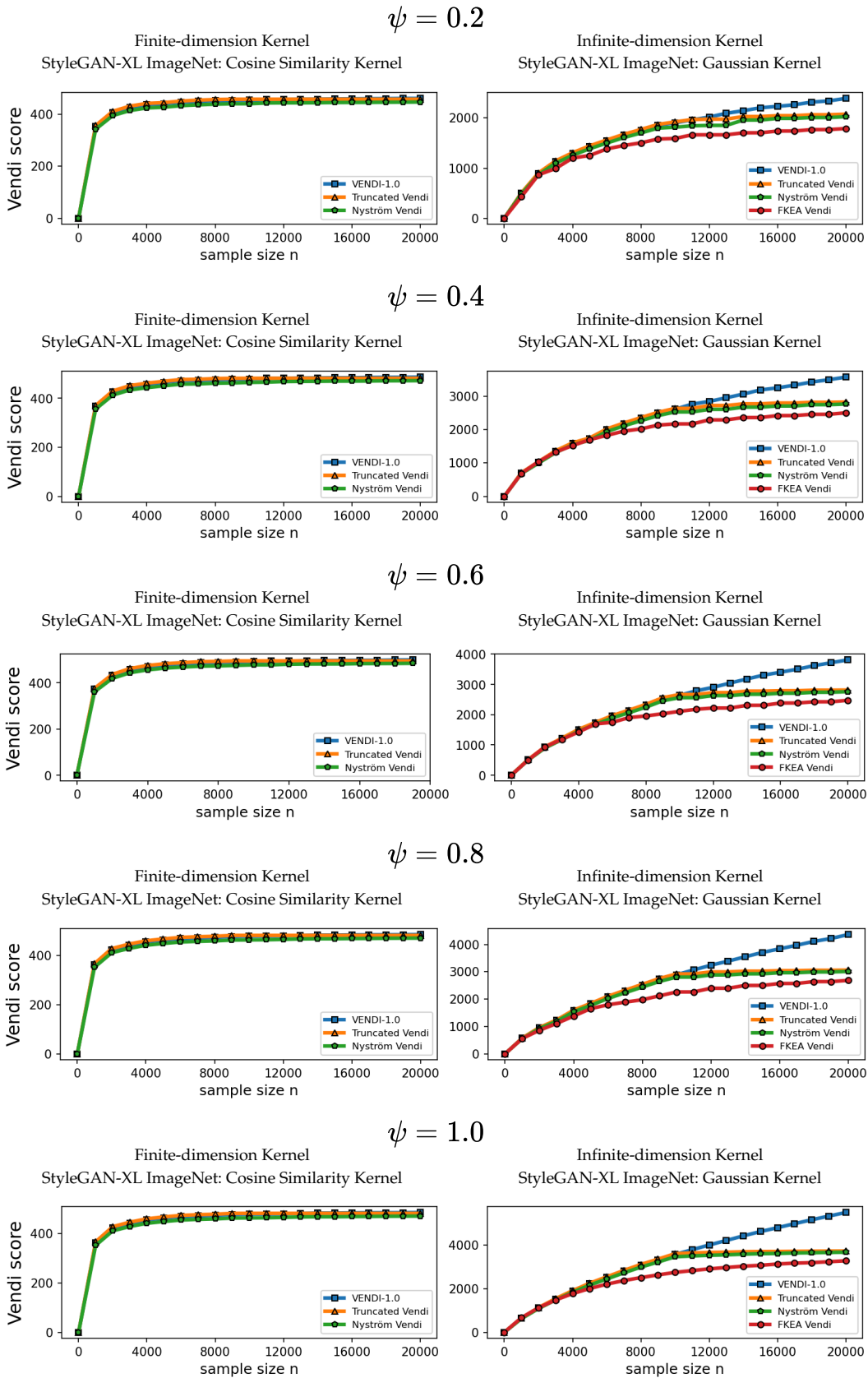


Figure 10: Statistical convergence of Vendi score for different sample sizes on StyleGAN-XL generated ImageNet data: (Left plot) finite-dimension cosine similarity kernel (Right plot) infinite dimension Gaussian kernel with bandwidth $\sigma = 40$. *DinoV2* embedding (dimension 768) is used in computing the scores.

B.1 Approximation error of VENDI scores

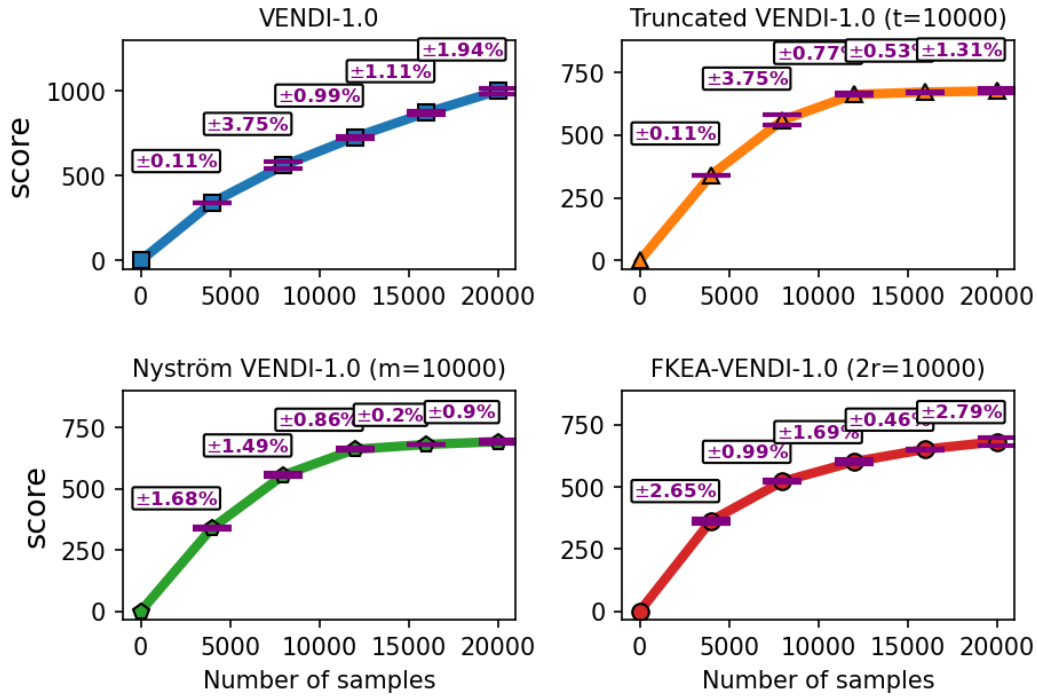
In this section, we demonstrate the numerical stability of all Vendi score variants. Figure 11 presents the standard deviation (expressed as a percentage) across varying sample sizes. The results indicate that, for each sample size n , the metric exhibits relatively low variance when computed across multiple sample sets drawn from the same underlying distribution, highlighting the robustness of the Vendi score computation. We present the results for ImageNet and FFHQ datasets.

B.2 Bandwidth σ Selection

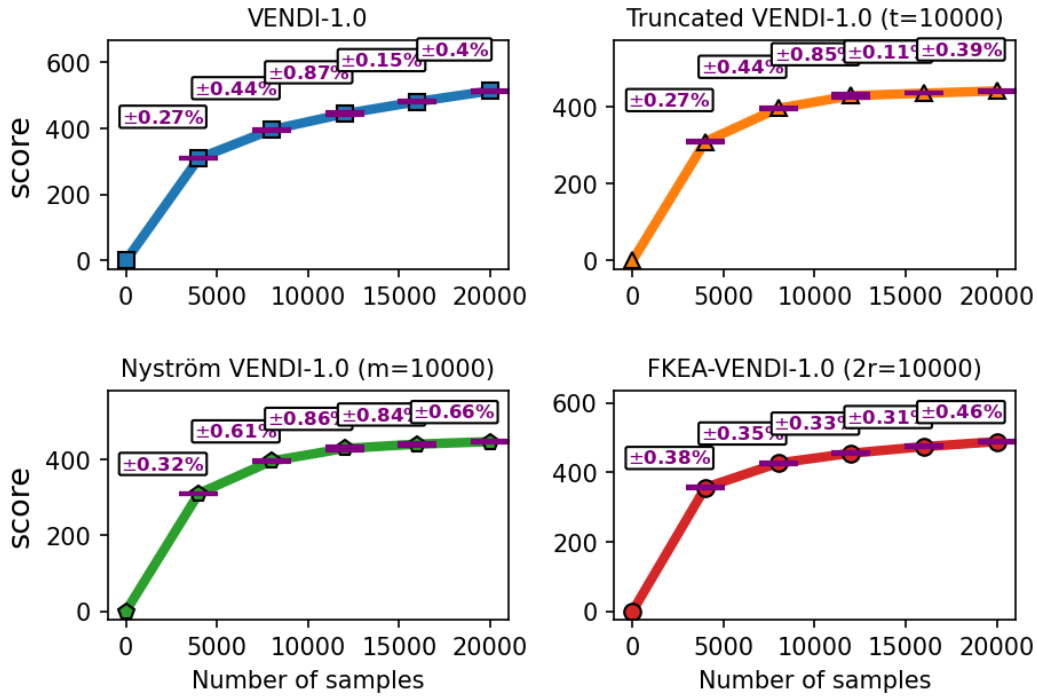
In our experiments, we select the Gaussian kernel bandwidth, σ , to ensure that the Vendi metric effectively distinguishes the inherent modes within the dataset. The kernel bandwidth directly controls the sensitivity of the metric to the underlying data clusters. As illustrated in Figure 7, varying σ significantly impacts the diversity computation on the ImageNet dataset. A smaller bandwidth (e.g., $\sigma = 20, 30$) results in the metric treating redundant samples as distinct modes, artificially inflating the number of clusters, which in turn slows down the convergence of the metric. On the other hand, large bandwidth results in instant convergence of the metric, i.e. in $\sigma = 60$ $n = 100$ and $n = 1000$ have almost the same amount of diversity.

C Selection of Embedding space

To show that proposed truncated Vendi score remains feasible under arbitrary embedding selection, we conducted experiments from Figures 3 and 4. Figures 12, 13, 14 and 15 extend the results to CLIP [24] and SWaV [37] embeddings. These experiments demonstrate that FKEA, Nyström and t -truncated Vendi correlate with increasing diversity of the evaluated dataset. We emphasize that proposed statistic remains feasible under arbitrary embedding space that is capable of mapping image samples into a latent space.



(a) ImageNet



(b) FFHQ

Figure 11: Statistical convergence of Vendi scores on image datasets with error bars. At each point we report percentage standard deviation across 10 independent metric computations.

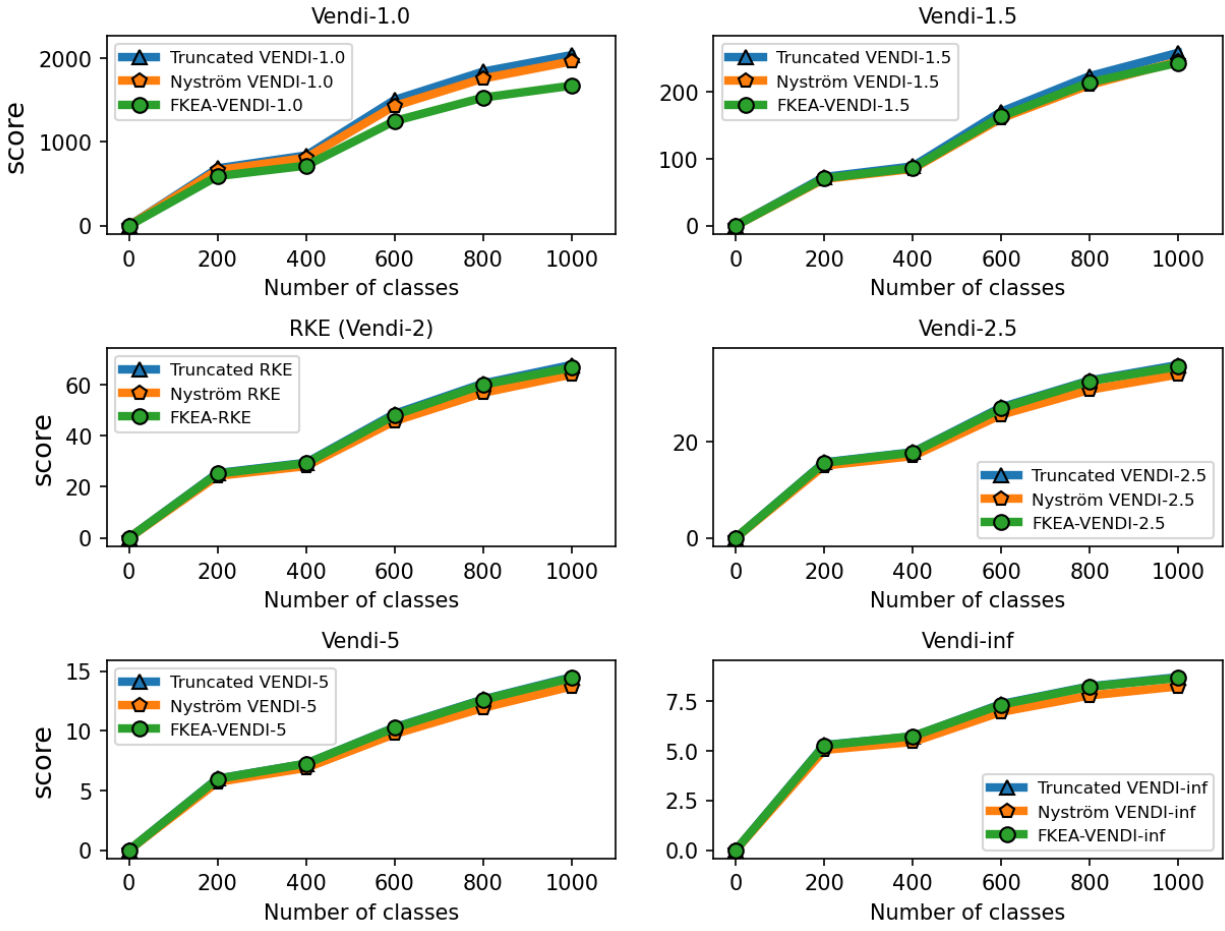


Figure 12: Diversity evaluation of Vendi scores on ImageNet dataset with varying number of classes based on *CLIP* embedding and bandwidth $\sigma = 5.0$

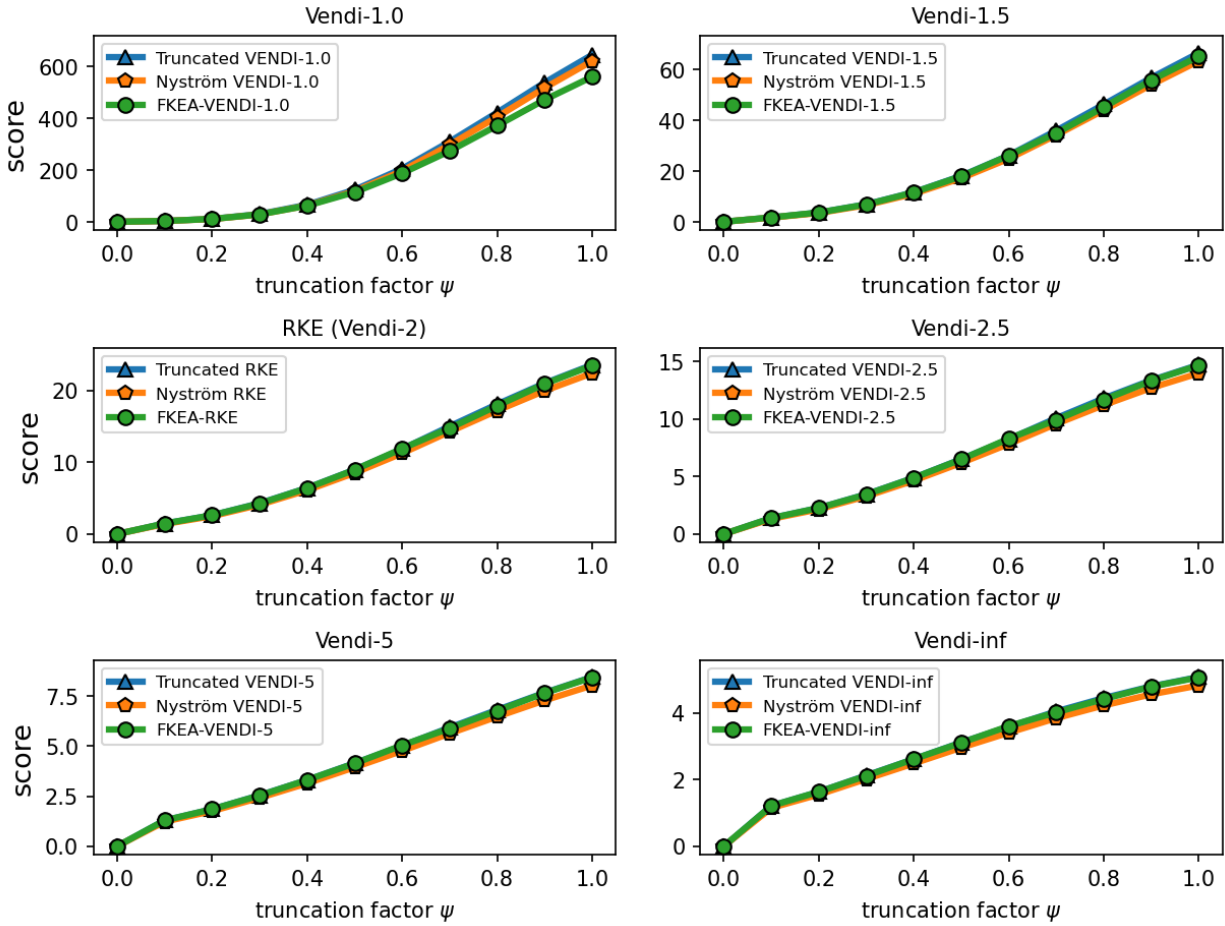


Figure 13: Diversity evaluation of Vendi scores on truncated StyleGAN3 generated FFHQ with varying truncation coefficient ψ based on *CLIP* embedding and bandwidth $\sigma = 5.0$

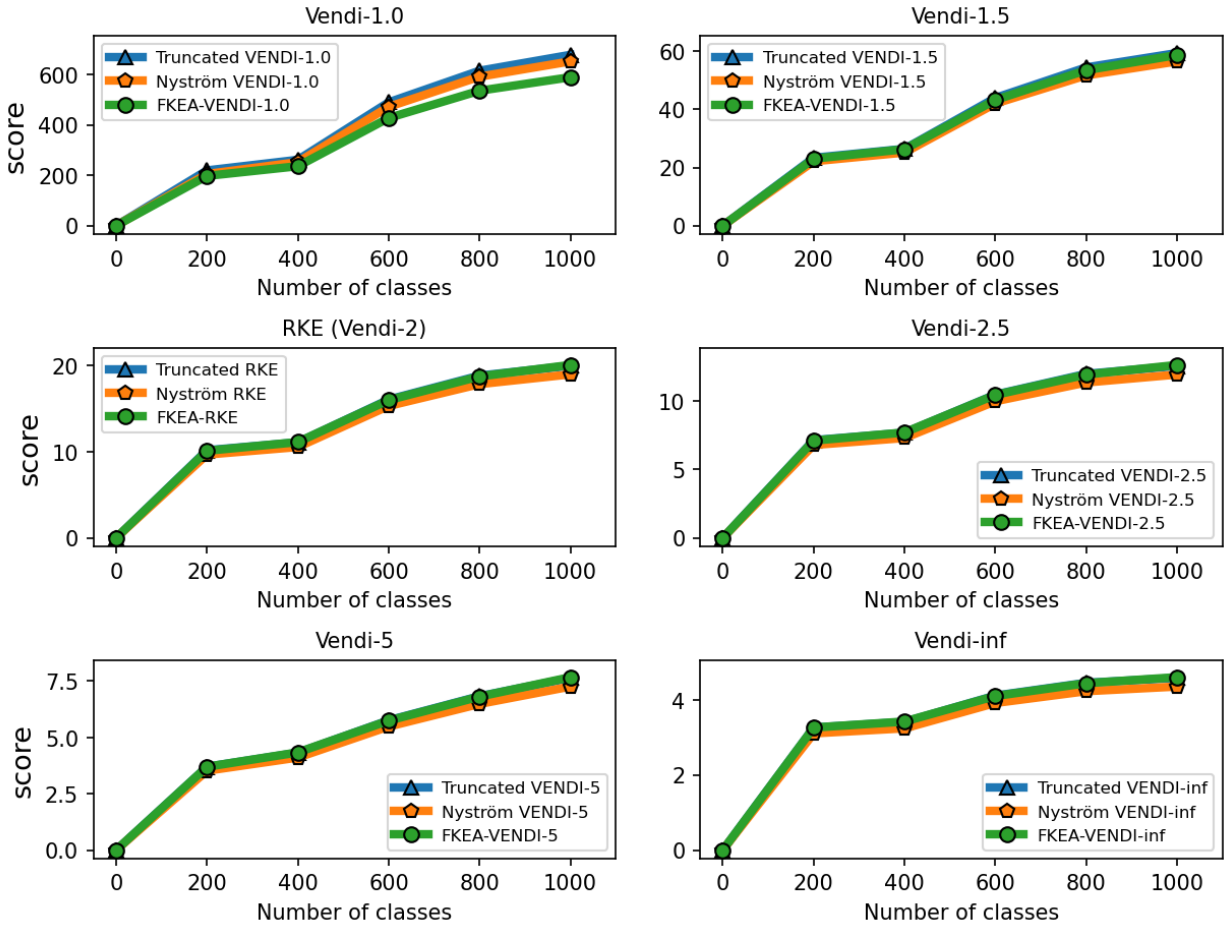


Figure 14: Diversity evaluation of Vendi scores on ImageNet dataset with varying number of classes based on *SWaV* embedding and bandwidth $\sigma = 1.0$

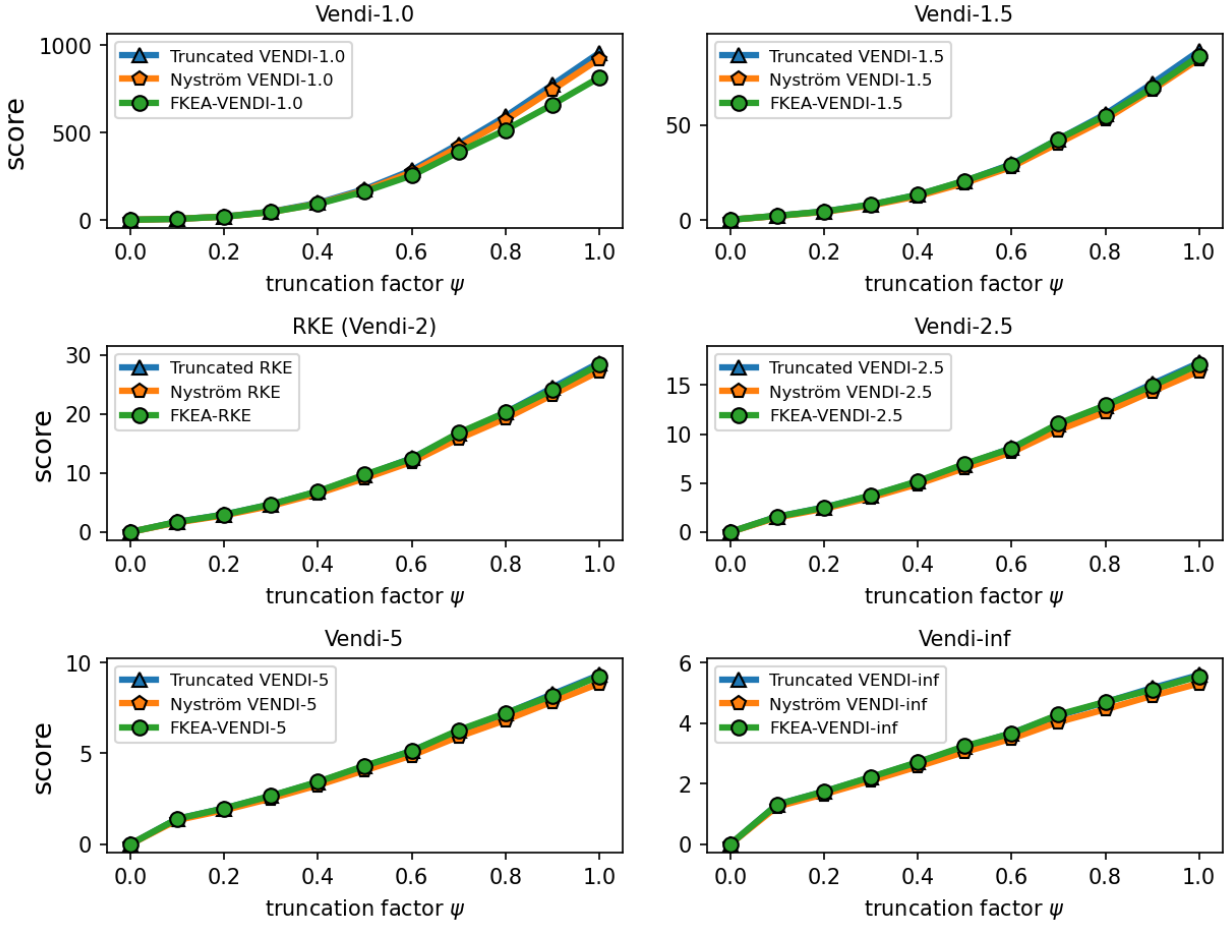


Figure 15: Diversity evaluation of Vendi scores on truncated StyleGAN3 generated FFHQ with varying truncation coefficient ψ based on $SwAV$ embedding and bandwidth $\sigma = 1.0$